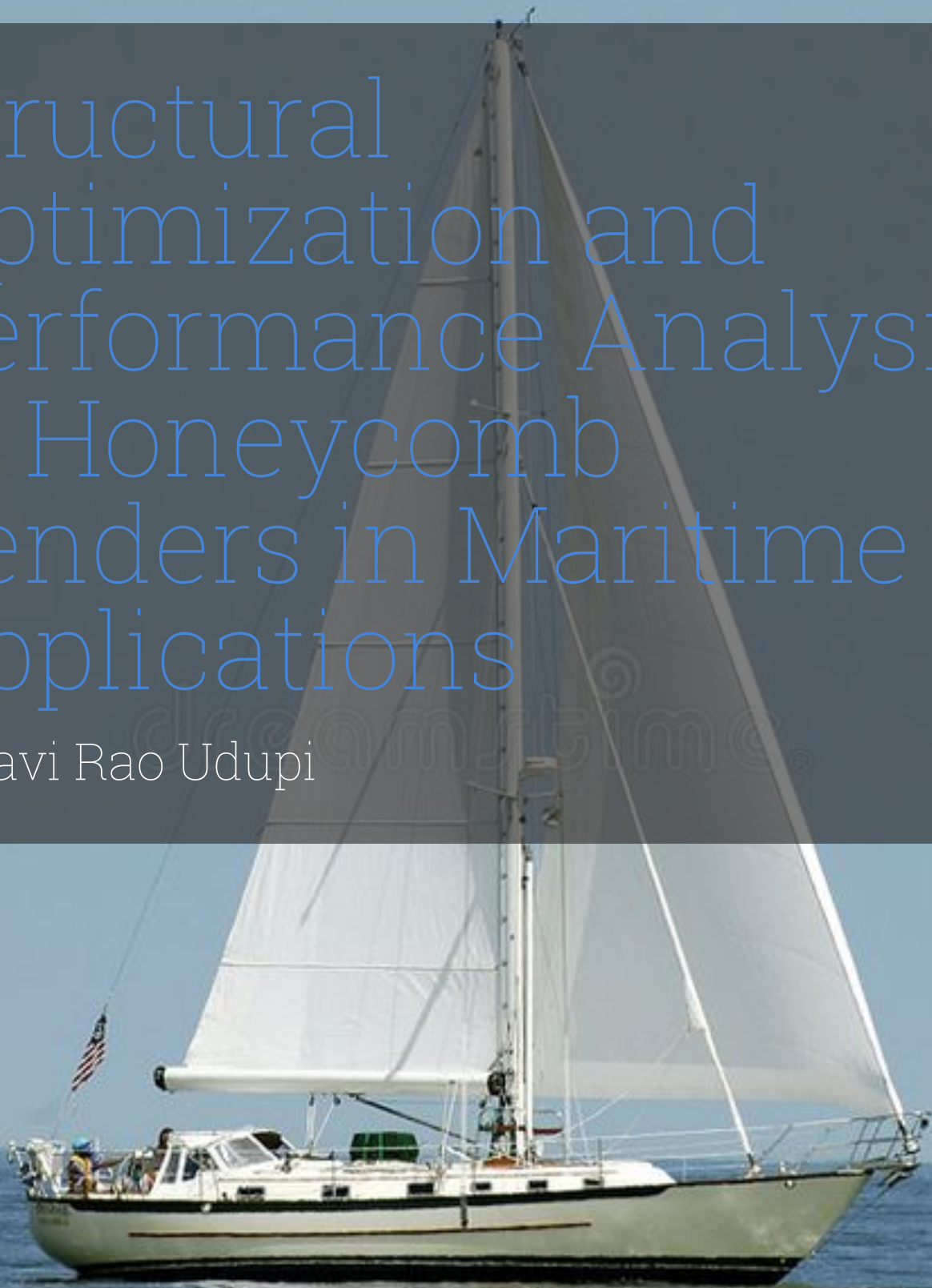


# Structural Optimization and Performance Analysis of Honeycomb Fenders in Maritime Applications

Pallavi Rao Udupi



# Structural Optimization and Performance Analysis of Honeycomb Fenders in Maritime Applications

by

Pallavi Rao Udupi

Pallavi Rao U 5758424

Supervisor: Dr. Jovana Jovanova  
Daily Supervisor: Amy Thomas  
Project Duration: 03, 2024 - 09, 2024  
Faculty: Faculty of Mechanical Engineering, Delft

Cover: <https://www.dreamstime.com/stock-images-boat-water-vertical-image17724>  
Style: TU Delft Report Style, with modifications by Daan Zwan-  
veld

# Abstract

This thesis investigates the enhancement of energy absorption in traditional PVC air-filled boat fenders through the incorporation of twisted honeycomb lattice structures. The research addresses critical deficiencies in existing fender designs, primarily focusing on improving energy dissipation consistency and reliability. By leveraging advanced metamaterial design principles, this study explores the impact of various twist angles applied to honeycomb configurations within the fender. Results indicate that a  $20^\circ$  twist maximizes energy absorption due to optimal stress distribution and synergy between compression and shear forces. Conversely, higher angles such as  $30^\circ$ , while initially improving energy absorption, introduce substantial stiffness, compromising the efficiency of energy distribution across the structure. This phenomenon underscores the importance of selecting appropriate twist angles to balance structural flexibility and energy management. The study employs ANSYS Workbench for explicit dynamic simulations to evaluate the performance of various configurations, confirming a structural activation threshold at  $10^\circ$ . This research advances the development of innovative fender designs, providing significant implications for their practical application in the marine industry.

# Acknowledgement

I would like to express my deepest gratitude to my supervisors, Dr. Jovana Jovanova and Amy Thomas, for their continuous guidance, encouragement, and invaluable insights throughout the course of this research. Their expertise and support were instrumental in shaping this project, and I am deeply appreciative of their mentorship.

I would also like to thank the faculty and staff of the Mechanical Engineering Department at TU Delft for providing an inspiring academic environment and access to the resources necessary for this work.

Finally, I extend my heartfelt thanks to my family and friends for their unwavering support and encouragement throughout my master's journey.



# Contents

<b>1</b>	<b>Introduction</b>	<b>1</b>
1.1	Background and Motivation . . . . .	1
1.2	Problem Statement . . . . .	2
1.2.1	Objectives . . . . .	2
1.2.2	Research Significance . . . . .	3
1.3	Scope of the Study . . . . .	3
<b>2</b>	<b>Literature Review</b>	<b>5</b>
2.1	History And Evolution of Boat Fenders . . . . .	5
2.2	Overview of Traditional Air-filled Fenders . . . . .	6
2.3	Energy Absorption Mechanism . . . . .	6
2.3.1	Basic Principles of Energy Absorption . . . . .	7
2.4	Biomimicry in Design . . . . .	8
2.4.1	Cellular Materials . . . . .	9
<b>3</b>	<b>Methodology</b>	<b>11</b>
3.1	Initial Design Considerations . . . . .	11
3.1.1	Base Fender . . . . .	12
3.1.2	Test Samples . . . . .	13
3.2	Simulation Setup . . . . .	16
3.2.1	The Courant–Friedrichs–Lewy (CFL) condition . . . . .	17
3.2.2	Constraints and Boundary Conditions . . . . .	18
3.2.3	Loads . . . . .	19
3.2.4	Contact Regions and Body Interactions . . . . .	19
3.3	Key Performance Metrics . . . . .	20
<b>4</b>	<b>Results</b>	<b>22</b>
4.1	Results of the base fender . . . . .	22
4.2	Dual-Method Energy Absorption . . . . .	24
4.3	Enhanced Dual-Method Energy Absorption . . . . .	25
<b>5</b>	<b>Discussions</b>	<b>31</b>
5.1	Interpretation of the results of the twisted structures . . . . .	31
5.2	Limitations . . . . .	32
5.3	Future Work . . . . .	33
<b>6</b>	<b>Conclusion</b>	<b>35</b>
	<b>References</b>	<b>36</b>
<b>A</b>	<b>Calculation</b>	<b>39</b>
<b>B</b>	<b>Energy Equations</b>	<b>40</b>
<b>C</b>	<b>Documentation of Experimental Observations and Rejected Design Concepts</b>	<b>41</b>
C.1	Monitoring and Analysis of Energy Metrics . . . . .	43
C.2	Rationale for Circular Cross-Section . . . . .	43

# 1

## Introduction

### 1.1. Background and Motivation

In maritime operations, fenders play a crucial role as protective buffers between ships and docking facilities or between two vessels. Their main function is to prevent damage to both the vessels and the dock by absorbing the impact and energy generated during berthing and mooring, which involves considerable motion and force [1]. By dispersing these forces, fenders help reduce the risk of structural damage and maintain the integrity of the vessels and infrastructure.

Traditionally, fenders are manufactured from materials such as foams, rubber, and air-filled PVC(Polyvinyl chloride) [2]. These materials have been favored for their initial effectiveness in energy absorption [3]. However, they often face limitations, such as plastic deformation and wear under extreme stress conditions, which lead to increased waste and frequent replacement cycles [4]. Moreover, PVC-based air-filled fenders, despite their prevalence, demonstrate inconsistency in energy absorption performance due to insufficient energy dissipation, highlighting a significant research gap in the field [5][6].

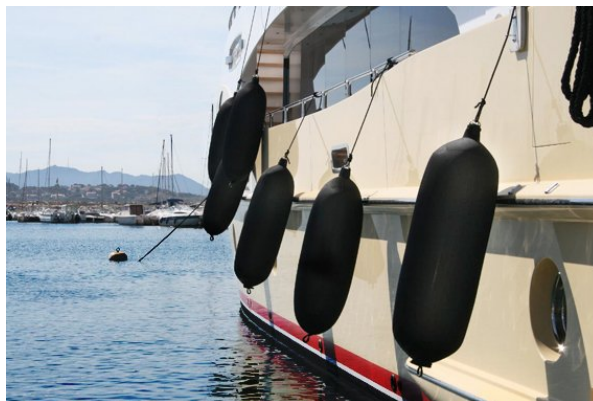


**Figure 1.1:** Figure depicting a fender suspended by a rope[7]

Central to the effectiveness of fenders is their ability to absorb energy efficiently, achieved through various designs and materials that enhance their performance under dynamic loads. Traditional fender materials, while initially effective, often struggle to maximize energy absorption efficiency. This challenge has spurred growing interest in advanced materials and designs,

such as metamaterials. Metamaterials leverage engineered microstructures to exhibit unique properties, such as enhanced toughness and a negative Poisson's ratio, not found in conventional materials [8].

Advancements in materials science and engineering have highlighted the potential of metamaterials, specifically those employing honeycomb lattice structures. These innovative designs offer enhanced energy absorption and structural integrity, providing an opportunity to overcome the deficiencies of traditional fenders by improving post-impact recovery capabilities and reducing environmental footprints through decreased material waste[9].

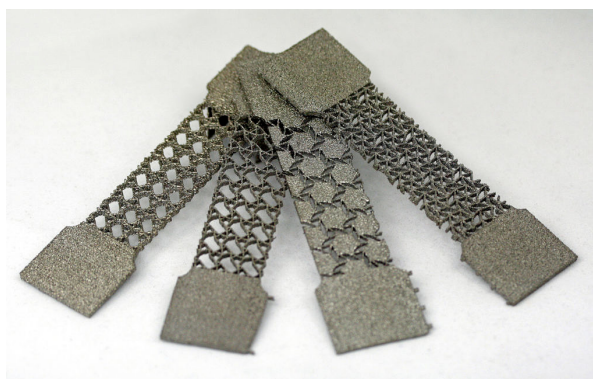


**Figure 1.2:** Figure showing cellular metamaterials[10]

The motivation for this project arises from the necessity to enhance the durability and efficiency of maritime fender systems amidst increasing demands on marine vessels. By integrating honeycomb lattice structures within PVC fenders, this project aims to leverage meta-material benefits to achieve superior energy absorption and durability. This integration not only addresses current performance variability and promotes longer service life but also seeks to minimize the stress transmitted to the hull of the boat during berthing and mooring operations.

## 1.2. Problem Statement

This study aims to enhance the performance of traditional air-filled boat fenders by exploring the potential of honeycomb lattice structures to improve energy absorption while using the same common material, PVC. The core problem can be defined as follows:

*The marine industry largely relies on boat fenders made from materials like foam, rubber, and air-filled PVC. However, these fenders often face issues such as plastic deformation under stress, leading to waste and high replacement costs. Additionally, inconsistent energy absorption and dissipation in PVC fenders result in performance variability. This research aims to address these challenges by exploring honeycomb lattice structures in PVC fenders, focusing on design improvements to enhance energy absorption, durability, and sustainability.*

### 1.2.1. Objectives

The objective of this report is to design and model alternative lattice-based fender structures, including honeycomb configurations and hybrid designs that combine air-filled and honeycomb elements, with PVC as the primary material. These designs will be explored through simulations to assess their potential for enhanced energy absorption. Additionally, comparative performance evaluations will be conducted using simulations. These simulations will analyze the energy absorption efficiency and durability of the newly designed hybrid honeycomb PVC

fenders in comparison to traditional air-filled PVC fenders, under controlled virtual testing conditions.

### 1.2.2. Research Significance

By optimizing the design of fenders while retaining PVC as the base material, this project aims to reduce long-term costs associated with fender maintenance, and improve the overall resilience of boats and yachts during docking and mooring processes.

### Research Questions

- How do lattice structures, such as honeycomb designs, compare to traditional air-filled PVC fenders in terms of energy absorption capabilities?
- Can the energy absorption of PVC fenders be improved solely through design optimization without changing the material?
- Does incorporating honeycomb structures within a traditional air-filled fender enhance its energy absorption capabilities?
- What impact does twisting the honeycomb structures have on energy absorption, and is there an optimal angle for this twist?
- Is there a trend in energy absorption relative to changes in the angle of twist?

## 1.3. Scope of the Study

This study aims to investigate the potential advantages of replacing traditional inflatable boat fenders with innovative honeycomb structures created using PVC. The scope of this research includes various critical factors such as design and simulation of both fender types, focusing on their application in marine environments.

The scope of this study specifically includes two types of fenders:

- **Traditional Inflatable Fenders:** These widely used fenders rely on air-filled designs that absorb kinetic energy during impacts through air compression. The research will evaluate their energy absorption characteristics and any limitations that arise from using this design.
- **Lattice Structures:** Bio-inspired and innovative hybrid honeycomb designs, also constructed from PVC, will be modeled to assess their potential as an efficient alternative to traditional inflatable fenders. The study will analyze the structural integrity and energy absorption capabilities of the innovative honeycomb design.

### Materials Consideration:

Manufacturers commonly choose PVC for inflatable fenders due to its beneficial properties. It is exceptionally durable, making it resistant to the demanding maritime environment, including exposure to UV rays, saltwater, and temperature changes. PVC's strong chemical resistance also allows it to withstand contact with oils and other chemicals frequently encountered during shipping. Additionally, PVC offers an ideal mix of flexibility and toughness, which helps fenders absorb and distribute impact energy efficiently without cracking. Its lightweight nature further simplifies fender handling and installation, and it remains an affordable material compared to other options used in similar applications [11][12].

In this study, taking into account the reasons mentioned previously, PVC will remain the consistent material utilized for both traditional inflatable and honeycomb fender designs. The emphasis will be on optimizing various parameters, including the geometric configuration of the

honeycomb structures and experimenting with different design parameters like twist angles, the overall outer cross-section of the fender itself, etc to enhance overall performance.

**Design and Modeling:**

Both the base model, which replicates the traditional air-filled fender, and the various sample models used for comparison to determine the optimal design were developed using Solid-Works.

- **Engineering Design Parameters:** The scope will include determining optimal configurations, cell geometries, and wall thicknesses to maximize energy absorption.
- **Cross-Sectional Design:** Only the cross-sectional profiles of the fenders will be designed and modeled rather than the entire fender. This approach aims to simplify the analysis process and reduce the time required for simulations while still allowing for effective evaluation of performance characteristics.

**Simulation:**

A critical component of this study will involve simulating the performance of both fender types using ANSYS Workbench. The study will establish simulation protocols to recreate real-world impact scenarios, allowing a systematic assessment of energy absorption, deformation, and overall structural performance. Simulation results will provide quantitative data regarding the reaction forces, deformations, and energy absorption for both fender designs, facilitating a comprehensive performance analysis.

# 2

## Literature Review

### 2.1. History And Evolution of Boat Fenders

The evolution of boat fenders represents a significant advancement in maritime safety, designed specifically to reduce collision damage during vessel docking and mooring. Initially made from woven ropes and natural fibers, early fenders acted as crucial barriers between ships and docks, primarily relying on their physical mass to absorb impacts. However, with the increase in maritime traffic and the growth of larger vessels, the demand for more effective energy absorption solutions became essential [13].

The emergence of synthetic materials in the 20th century brought about a revolutionary change in fender technology. The introduction of rubber and plastic materials allowed for enhanced energy absorption and durability, leading to the widespread adoption of more sophisticated fender designs, such as cylindrical, D-shape, and arch fenders[14]. These designs emerged as prevalent options, each offering unique impact absorption characteristics tailored to different vessel types and docking circumstances[15].

Engineering advancements have not only targeted enhancements in materials but also the innovative geometric configurations of fenders. This evolution in understanding the intricacies of berthing energy underscores the importance of refining fender systems to effectively absorb significant amounts of this energy [16].

Today's fender designs reflect a blend of historical practice and modern engineering capability, with an emphasis on materials and configuration factors like the eccentricity, virtual mass, configuration, and softness coefficients, underscoring their critical roles in energy dissipation[17]. As maritime technologies evolve, the fundamental purpose of fenders remains unchanged: to protect both the vessel and docking infrastructure by effectively managing the forces involved during vessel berthing.



(a)



(b)

**Figure 2.1:** Figure illustrating rubber and rope fenders respectively(Photo by Author)

## 2.2. Overview of Traditional Air-filled Fenders

Pneumatic fenders function by leveraging compressed air as a cushioning medium, providing a protective barrier that reduces collision risks, which can otherwise result in significant damage. These fenders can handle various compression scenarios, such as the normal and angular compression. This means they can withstand pressures from different angles and intensities, which is critical for protecting ships during docking [18].

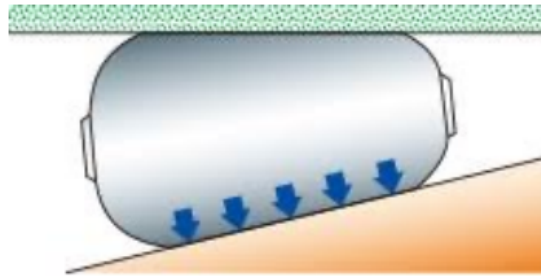


**Figure 2.2:** Illustration of the compression of an air-filled fender[19]

## 2.3. Energy Absorption Mechanism

Increasing awareness and the legal implications of mechanical failures underline the necessity for advanced passive safety measures in various fields. This mandates a thorough understanding of energy-absorbing structures and materials, particularly due to their effectiveness in dissipating kinetic energy during impact or dynamic loading. Such research has been prominent since the 1970s, especially in the automobile and military sectors [20]. Crashworthiness is the measure of how well a vehicle withstands and responds to impacts, aiming to minimize damage to both vehicle and occupants [21]. Conventional structures in civil engineering and machinery typically experience small elastic deformations under working loads and are designed for strength and stiffness to avoid fatigue, corrosion, or material degradation over time. In contrast, energy-absorbing structures must endure intense impact loads, leading to large geometry changes, strain-hardening effects, strain-rate effects, and interactions between different deformation modes such as bending and stretching [22].

### 2.3.1. Basic Principles of Energy Absorption

Design and material selection for energy-absorbing structures aim to control kinetic energy dissipation effectively. Fundamental principles include:

- **Irreversible Energy Conversion:** Energy should be converted into inelastic forms such as plastic deformation or other dissipative mechanisms (e.g., friction or fracture) to prevent energy storage and subsequent release, which could aggravate damage. Imagine a sailboat crashing into a large elastic spring. Initially, the spring compresses as seen in figure 2.3, slowing down the sailboat as its kinetic energy is transferred into the elastic strain energy of the spring. Once the spring has compressed as much as possible, it begins to return to its original shape. During this recovery, the spring accelerates the sailboat as shown in figure 2.4, converting the stored elastic strain energy back into kinetic energy. This process subjects the sailboat's occupants to intense deceleration followed by intense acceleration. Such forces can have serious consequences[22].
- **Long Stroke:** When designing energy-absorbing structures, the force,  $F$ , exerted needs to be controlled and consistent. This consistency is crucial as the work done,  $W$ , by the force is determined by multiplying the force's magnitude and the displacement  $d$ , along the direction of the force application. Therefore, a longer displacement (stroke) enables the structure to absorb more energy. The effectiveness of an energy-absorbing structure is often evaluated by the ratio of the stroke to the characteristic dimension. In some applications like packing fragile goods, the ratio,

$$\Delta_{max}/H \quad (2.1)$$

where  $\Delta_{max}$  is the deformable distance and  $H$  is the original material dimension, is critical. The ratio indicates compressibility and structures that exhibit significantly higher  $\Delta_{max}/H$  ratio usually absorb more energy efficiently[22].

- **Light Weight and High Specific Energy-Absorption Capacity:** Energy-absorbing components must be lightweight, with high specific energy-absorption capacities. Cellular materials like polymer foams and aluminium honeycombs are preferred due to their high compressibility and relatively low density [23].
- **Consistent and Reproducible Deformation Mode:** In order to address highly uncertain working loads, the deformation mode and energy absorption capacity of the designed structure must be consistent and reproducible, ensuring the reliability of the structure during its operation. It is essential to recognize that external dynamic loads applied to energy-absorbing structures and materials can vary significantly in terms of magnitude, pulse shape, direction, and distribution[22].



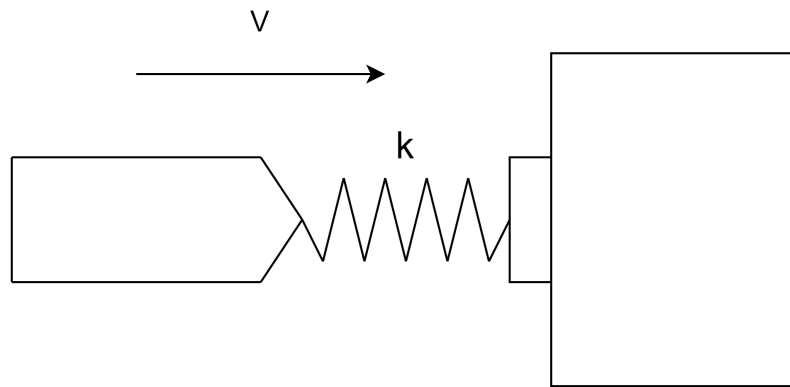


**Figure 2.3:** Figure showing compression of the spring when the boat hit the dock

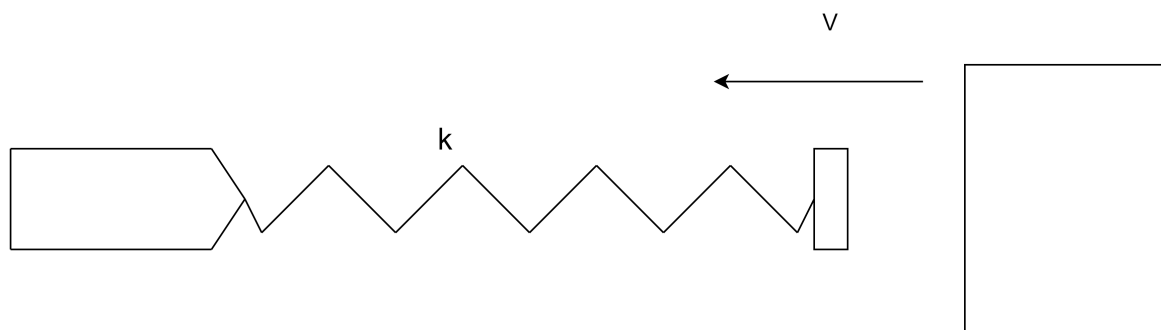


**Figure 2.4:** Figure showing the spring accelerating the boat

## 2.4. Biomimicry in Design

In the context of biomimicry, natural systems serve as a source of inspiration for developing cutting-edge engineering solutions. This project draws on the sophisticated overlapping scales of the pangolin and the spiral structure of eland horns to inform its design.

The spiral horns of the eland (*Taurotragus oryx*) offer a valuable model for biomimicry in impact-absorbing designs. These twisted horns are a vital evolutionary adaptation for combat. Male elands use their spiraled horns to interlock with opponents, reducing direct high-impact forces by encouraging a twisting, grappling movement rather than a full-force collision [24]. This design distributes stress more evenly along the horn, minimizing damage and protecting the skull from significant impact [25].

Pangolin scales, notable for their toughness, serve as a defensive adaptation, forming overlapping armor when the animal curls into a ball[26]. They are composed of both  $\alpha$ - and  $\beta$ -keratins, forming a crossed-lamellar structure capable of absorbing impacts from various angles [27]. This structural characteristic allows pangolin scales to exhibit a uniform response to tensile stress regardless of orientation, maintaining mechanical strength with a degree of elasticity [27]. The scales' ability to deform without fracturing under compressive forces further illustrates their capacity for energy dissipation and toughness[28].



**Figure 2.5:** Image depicting a Pangolin rolled into a ball [29]

Further, in pangolin scales, the keratin lamellae are nearly parallel to the exterior surface but gradually tilt to approximately  $45^\circ$  toward the interior. This intentional misalignment with externally applied loads significantly improves strength and stiffness. It achieves this by promoting fracture resistance through crack deflection mechanism[30].

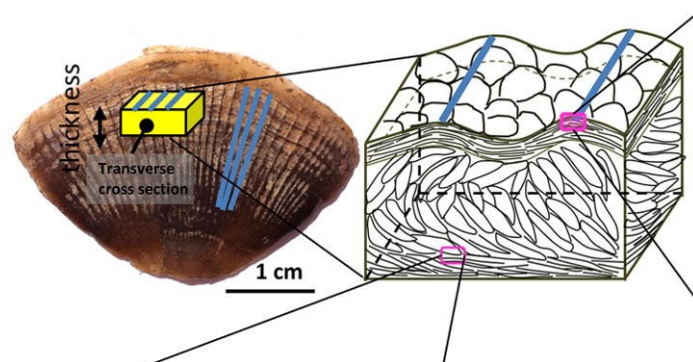


**Figure 2.6:** Figure of keratin lamellae twist [31]

Additionally, throughout history, honeycomb structures have been inspired by nature. For instance, as seen in bee hives, the classical hexagonal configuration is designed for optimal space utilization, using minimal material (beeswax), a concept known as the honeycomb conjecture[32]. This natural efficiency inspired advancements in human-engineered honeycombs, leading to their application in diverse fields such as architecture, automotive, aerospace, and electronics [33].

#### 2.4.1. Cellular Materials

Cellular materials like foams and honeycombs are emerging as a new class of lightweight, high-performance materials[34]. They have excellent energy-absorption properties, and their study is essential for various structural applications. Honeycombs are highlighted as typical examples of cellular materials and are often used as core structures in sandwich panels for their energy-absorbing capabilities [35]. The cell structure of honeycombs predominantly features

hexagonal sections, but can also include other shapes such as triangular, square, rhombic, or circular [36].

These materials can be characterized by spatially varied microstructures, allowing for non-uniform distribution of reinforcement phases across different properties, sizes, and shapes, or by continually interchanging the roles of reinforcement and matrix phases [34]. The flexibility in manipulating micro-scale parameters such as density, cell wall, and face thickness allows these materials to be engineered for optimal energy absorption and efficiency, making them promising candidates for advanced structural designs [37].

Honeycomb structures in particular are characterized by their two-dimensional, periodic arrangement of unit cells, forming a lightweight and highly porous architecture [38]. The topology of repeating unit cells significantly impacts the mechanical performances of honeycombs, allowing for distinctive traits such as negative Poisson's Ratio (NPR), and negative stiffness [39]. These extraordinary properties arise from the material's micro structural design rather than the the intrinsic qualities of the matrix materials itself, which is why honeycombs exhibit superior performance in fracture toughness and impact resistance [33].

Classical honeycomb configurations, inspired by natural structures like beehives and developed for engineering applications, include a variety of micro-structural designs that have been extensively studied and applied. The hexagonal honeycomb, modeled after the efficient geometry of beehives, is among the earliest and most widely used configurations[33].

# 3

## Methodology

The methodology for this study is designed to evaluate the performance of traditional air-filled boat fenders versus the hybrid structures filled with both air and honeycomb structures made from PVC. This chapter outlines the design and modeling process, describes the simulation protocols used, and details the analysis methods employed to understand and optimize the energy absorption capabilities of these fender designs.

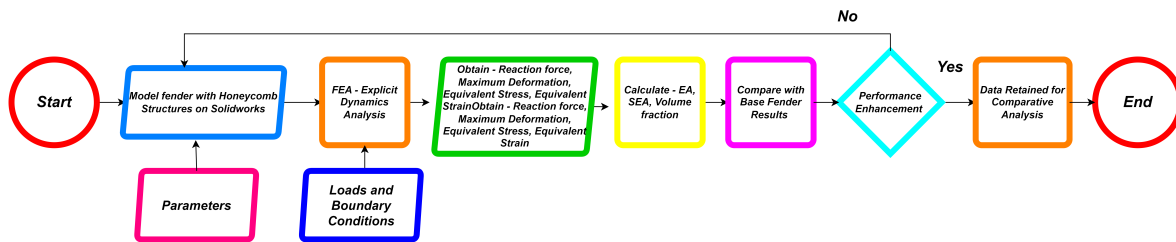


**Figure 3.1:** Overview of the Employed Design Process

### 3.1. Initial Design Considerations

The methodology employed for the performance evaluation of all fenders is consistent to ensure uniformity and comparability across different assessments. All the fender samples were constructed using SolidWorks. These models were then imported into ANSYS Workbench, where explicit dynamics simulations were conducted to test the samples. This approach allowed for the assessment of each fender's structural integrity and performance under various impact scenarios, ensuring that the designs could withstand realistic docking conditions and collisions, thereby validating their effectiveness and reliability.

The focus of the project is on structurally modifying the design to enhance energy absorption, rather than changing the material itself. By optimizing the fender's geometry and internal structure, improvements in impact resistance and load distribution can be achieved. Retaining PVC helps in clearly determining the impact of design changes by isolating them from material properties. The table below presents the properties of PVC as obtained from ANSYS Workbench:

<b>Density</b>	<b>Young's Modulus</b>	<b>Poisson's Ratio</b>	<b>Bulk Modulus</b>	<b>Shear Modulus</b>
$1.335 * 10^{-6} kg/m^3$	$32.4 MPa$	0.475	$216 MPa$	$10.983 MPa$

**Table 3.1:** Table presenting the properties of PVC

Further, the highest recorded berthing velocity is  $13 cm/s$ , equivalent to  $0.2527 kn$  [40]. For the purpose of this project, the velocity at which the fender strikes a fixed object, such as a dock or another boat, is assumed to be  $5 kn$ , considering worst-case scenario. Further, in realistic situations, even in controlled scenarios like docking, the boat is unlikely to impact at a perfect  $90^\circ$  due to the various docking methods employed, which are influenced by the current's nature at the time of docking. Therefore, impact angles of  $30^\circ$ ,  $45^\circ$ ,  $60^\circ$ , and  $75^\circ$ , in addition to a  $90^\circ$  impact angle, are considered to simulate both controlled and uncontrolled situations.

<b>Angles [°]</b>	<b>Corresponding Velocities [mm/s]</b>
30	1286.11
45	1818.83
60	2383.49
75	2484.57
90	2572.22

**Table 3.2:** A table listing the angle of impact along with the corresponding magnitude of velocity for each angle.

### 3.1.1. Base Fender

For the base fender seen in figure 3.2, a PVC sample was initially selected from a dealer's catalog [41]. To enhance efficiency and reduce computation time, a cross-section sample size of thickness  $5 cm$  was chosen for testing. This size was considered appropriate because it strikes a balance between being large enough to provide accurate insights how it deforms, yet small enough to facilitate quicker testing. Additionally, the selected fender has a diameter of  $25 cm$  and a length of  $80 cm$  [41]. These dimensions were specifically chosen because they represent a standard size commonly used in typical applications, ensuring that the test results would be broadly applicable and relevant for practical use.

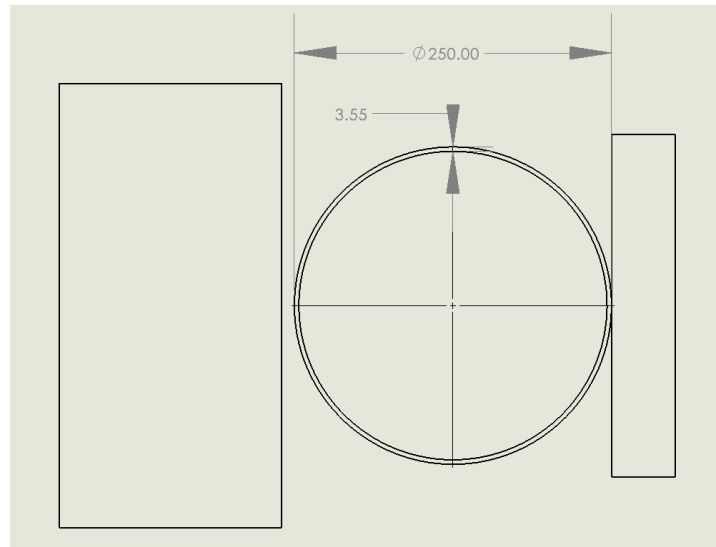


**Figure 3.2:** Diagram of a base fender with dimensions in mm

The entire fender weighs  $3kg$ , according to the catalog [41]. Assuming uniform geometry, 16 samples were derived from its  $80cm$  length, with each  $5cm(50mm)$  sample weighing approximately  $0.1875kg$ . To ensure accuracy in the SolidWorks model, the base fender was designed with a wall thickness of  $3.5mm$ , aligning the model's weight with that of an actual  $5cm$  fender sample.

Additionally, the internal air pressure exerted on the fender's wall was set to  $2psi(0.0137895MPa)$ , a value established by the fender manufacturers based on practical experience [42].

The primary mechanism behind air-filled fenders is air compression. When a boat impacts the fender, the air inside the fender compresses, allowing the fender to deform temporarily. This deformation helps dissipate the impact energy, preventing damage to both the boat and the dock.

### 3.1.2. Test Samples

The samples intended for testing and comparison against the base model were developed by maintaining the original external structure and integrating internal honeycomb structures as seen in figure 3.3 and 3.4. Initially, the base thickness was  $3.55mm$ . It has now been reduced to a wall thickness of  $2mm$ , with the honeycomb cell walls also measuring  $2mm$ . The honeycombs have a length of  $50mm$ .

The air within the structure is maintained at a consistent pressure of  $2psi$ , serving as the primary mechanism of energy absorption. As previously discussed, the compression of the air allows the structure to deform and absorb impact forces. With the addition of honeycomb structures, a secondary energy absorption method is introduced. With this combination of air compression and the honeycomb's mechanical resilience, the structure is expected to dissipate energy effectively making this test sample a **dual-method system** for impact absorption.

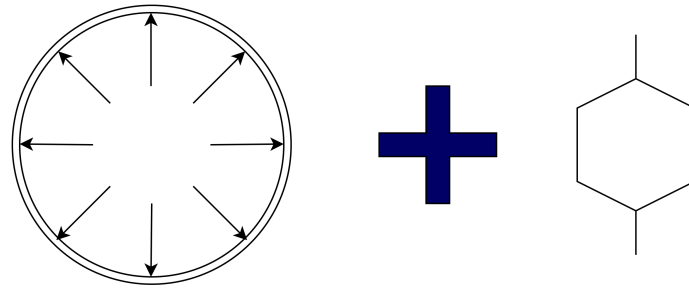


**Figure 3.3:** Diagram illustrating the integration of honeycomb unit cells into the base fender for the dual-method system

Further, keeping the external structure intact prevents various components from water bodies, such as debris and aquatic organisms, from getting stuck in the lattice structures. This ensures the fender remains functional and free from blockages that could compromise its performance. A thinner wall enhances the flexibility of the fender, enabling more effective energy absorption during impacts by allowing the outer structure to deform more efficiently and distribute stress across the honeycomb structure. Additionally, maintaining the original thickness of the base fender for the honeycomb structure would significantly increase the overall weight. Therefore, after careful consideration, a thickness of  $2mm$  was selected—striking a balance between being not too thin to compromise strength and not too thick to add to the weight.

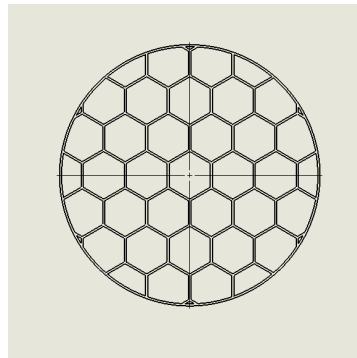


**Figure 3.4:** Illustration depicting a cross-sectional view of a traditional inflatable fender incorporating honeycomb structures

The final series of samples introduces varying twist angles, beginning at  $5^\circ$ , to explore the concept of an **enhanced dual-method** energy absorption. This design modification aims to enhance the fender's ability to absorb energy through a combination of mechanisms: deformation, and torsional effects as shown in figure.

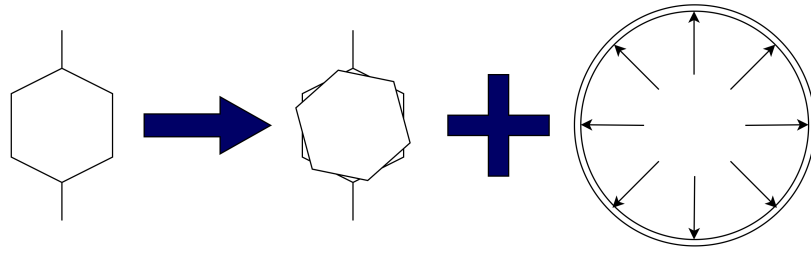


**Figure 3.5:** Diagram illustrating the integration of twisted honeycomb unit cells into the base fender for the enhanced dual-method system

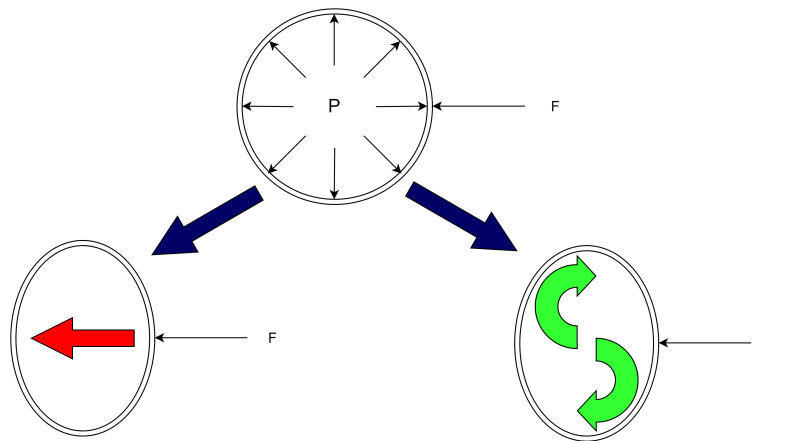


**Figure 3.6:** Diagram illustrating the expected internal mechanics within the fender that lead to deformation upon impact.

In the diagram 3.6, the compressed cross-section with the red arrow representing the direction of compression caused by internal air pressure, while the green arrows denote the torsional forces induced by the twisted honeycomb design. The primary method involves compression from the internal air, while the secondary mechanism leverages torsion generated by the twist in the honeycomb cells. This expected deformation of the structure is inspired by the misalignment observed in pangolin scales, which helps reduce crack propagation and, in turn, enhances the structure's longevity as mentioned in 2.

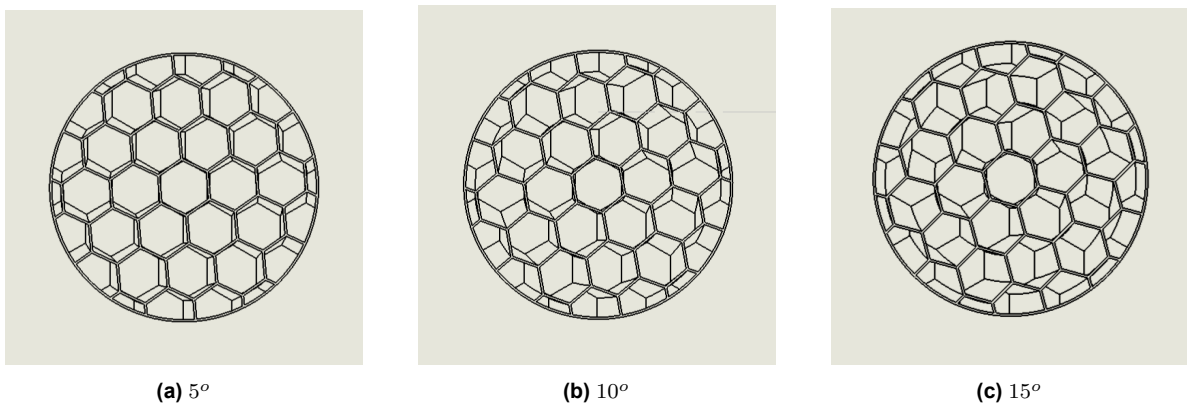


**Figure 3.7:** Figure illustrating the enhanced dual-method sample.



### 3.2. Simulation Setup

Explicit dynamics in ANSYS Workbench was utilized for the analysis. The explicit method is particularly effective for solving dynamic problems involving interactions of deformable bodies, especially in high-speed dynamic events. It allows for the simulation of complex transient phenomena with rapidly changing interactions and deformations, making it suitable for high-impact, high-speed events analysis. [43].

The following figure illustrates the simulation setup before impact, after impact, and finally the front view of the setup, respectively.

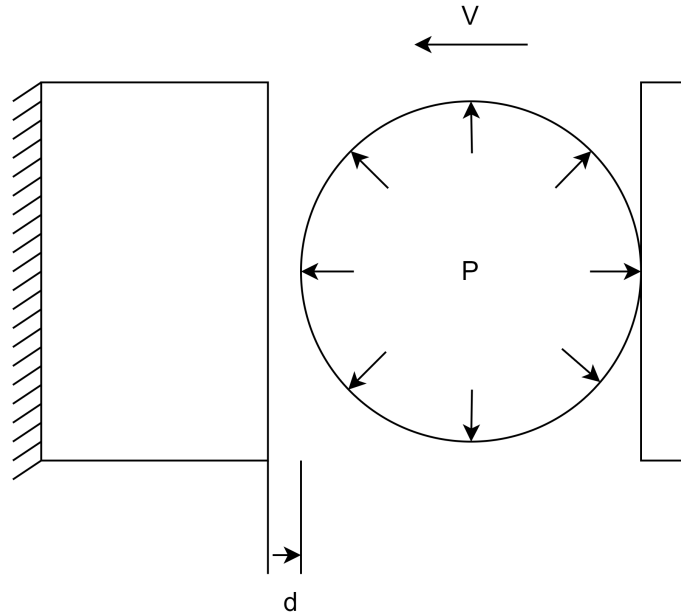


**Figure 3.8:** Diagram illustrating the setup before impact

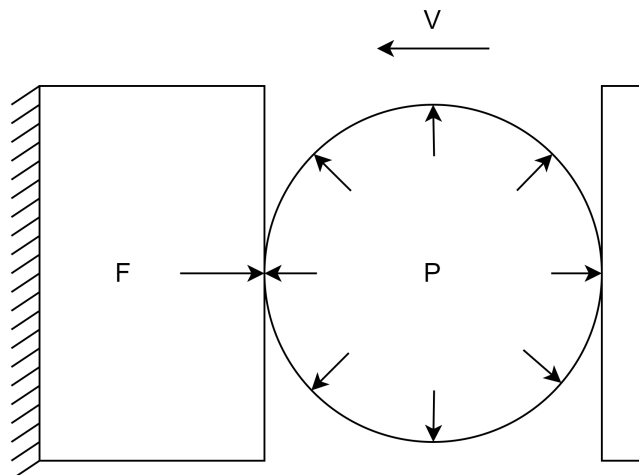


**Figure 3.9:** Diagram illustrating the setup after impact

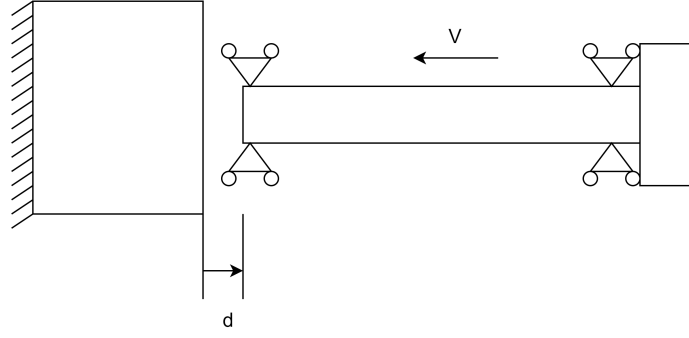


**Figure 3.10:** Diagram illustrating front view of the setup to show the displacement constraint

### 3.2.1. The Courant–Friedrichs–Lewy (CFL) condition

The Courant–Friedrichs–Lewy (CFL) condition is a critical concept in explicit dynamics, especially when using finite element methods for solving dynamic problems. It is a stability criterion that constrains the time step size for explicit integration schemes to ensure reliable and accurate results [44].

The CFL condition, shown in equation 3.1, states that the time step must be small enough so that a stress wave cannot travel more than one element length during a single time step [45]. This condition ensures numerical stability and accuracy of the simulation.

$$\Delta t < t_{crit} \quad (3.1)$$

where,  $t_{crit}$  is the time taken by the stress wave to travel through the smallest element.

$$t_{crit} = f * L/c \quad (3.2)$$

where,

$f$  is the scaling factor and  $f \leq 1$

$L$  is the characteristic length of the smallest element

$c$  is the speed of the sound in the material

The characteristic lengths of the elements differ among the various samples. Further,

$$c = \sqrt{E/\rho} \quad (3.3)$$

where,

$E$  is the Young's Modulus and for PVC,  $E = 32.4 \text{ N/mm}^2$

$\rho$  is the density and for PVC,  $\rho = 1.335 * 10^{-6} \text{ kg/m}^3$

For PVC, the calculated value of  $c$  is  $4926.424964 \text{ mm/s}$ .

Lastly, End time  $T$ , was set to  $1 \text{ s}$ . Setting the end time to 1 second for the explicit dynamics test of the fender samples is a strategic choice that balances capturing the relevant impact dynamics while maintaining computational efficiency. This duration is sufficient to observe the complete response of the fender to typical impact scenarios, including the initial contact

and the deformation. Additionally, this time setting ensures the simulation encompasses the essential behaviors without extending into unnecessary computationally intensive territories, enabling evaluation of performance within a practical and controlled simulation environment.

Therefore, calculating the number of cycles is a crucial "Analysis Setting", as this parameter significantly impacts stability and must be accurately determined and inputted. The value obtained for (n) represents the minimum number of cycles needed to satisfy the CFL condition. The number of cycles input cannot be less than those calculated for the corresponding sample.

$$n = T/\Delta t \quad (3.4)$$

<b>Sample Name</b>	<b>Number of Cycles n</b>
Base Fender	2340
Sample Honeycomb	6920
Sample Honeycomb twist 5°	5548
Sample Honeycomb twist 10°	7143
Sample Honeycomb twist 15°	7380
Sample Honeycomb twist 20°	11483
Sample Honeycomb twist 25°	8016
Sample Honeycomb twist 30°	6845
Sample Honeycomb twist 35°	7257
Sample Honeycomb twist 40°	9729

**Table 3.3:** Table showing the number of cycles for all tested samples.

### 3.2.2. Constraints and Boundary Conditions

**Fixed Support:** A fixed wall composed of structural steel was modeled at a distance of 10mm from the fender sample as seen in figure 3.8 to effectively simulate realistic impact conditions. Structural steel was chosen due to its high strength and rigidity, which provide a reliable and consistent surface for assessing the fender's impact resistance. The 10mm distance was selected to replicate a close-proximity scenario, allowing for a detailed analysis of the fender's ability to absorb energy upon contact. This setup ensures that the test accurately reflects the operational challenges the fender would face. Therefore, for the wall,

$$\begin{aligned} u_x &= u_y = u_z = 0 \\ \theta_x &= \theta_y = \theta_z = 0 \end{aligned}$$

**Displacement Constraints on Fender:** The displacement boundary condition was set to prevent movement in the direction of gravity, with a displacement value of zero shown in figure 3.10. This decision was made because the test involved a 5cm section of the fender, which

is part of a continuous structure both above and below the sample. Therefore, in a real-world scenario, the top and bottom surfaces of the fender would remain stationary with respect to vertical motion. By constraining these surfaces from moving up or down, the simulation accurately reflects the physical behavior of the complete fender, ensuring that the analysis focuses solely on the response to lateral forces and impacts. This boundary condition helps maintain the structural integrity and realistic deformation characteristics of the sample during testing. Therefore, for the fender,

$$u_y = 0$$

This is also periodic boundary condition, that guarantees that the top and bottom edges behave similarly, promoting consistency in the simulation. By enforcing this condition, we can accurately model the repetitive features of the fender, which is essential for understanding its overall performance under dynamic loading.

$$u_{top} = u_{bottom}$$

### 3.2.3. Loads

**Impact load calculations:** Calculating impact forces in dynamic situations can be quite complex, so an alternative approach involves considering the reaction force resulting from the specified velocity as an external force. This method simplifies the analysis by using the known velocity of the impacting object to estimate the forces exerted on the fender. By focusing on the reaction force, the analysis can accurately capture the stresses and energy absorption characteristics without directly calculating the intricate dynamics of the impact load itself. This approach helps streamline the process, providing meaningful insights into the fender's performance under specified conditions.

**Internal wall pressure:** Inflatable fenders are filled with air, which exerts pressure on the fender's walls. In the industry, it is recommended that this internal pressure,  $P$ , be set to  $2psi$ . This pressure setting ensures that the fender maintains its shape and provides optimal energy absorption during impact.

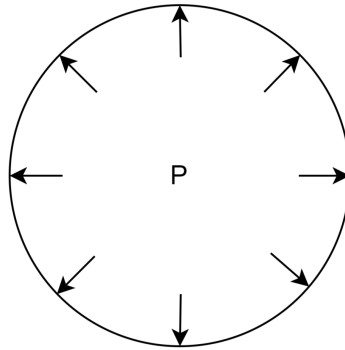


**Figure 3.11:** Diagram depicting the pressure exerted by air on the wall

### 3.2.4. Contact Regions and Body Interactions

**Contact Regions:** There is a contact region between the fender itself and a small cuboid modeled to emulate the boat structure, which is bonded. The bonded contact region likely represents areas of the assembly where parts are intended to remain rigidly connected, such as the attachment points of the fender to specific structural components. This setup ensures that these regions do not experience relative motion or separation.

**Body Interactions:** Friction-less interactions between the fender and the structure it crashes

into allow for the examination of the fender's mechanical response without the added complexity of frictional forces.

### 3.3. Key Performance Metrics

The key performance metrics stated below, serve as the foundational basis for comparing the base fender with various test samples, aiming to identify a sample that surpasses the base in performance. By comparing these metrics, it is possible to determine specific improvements or advantages demonstrated by the test samples. Ultimately, this approach guides the selection of a fender sample that provides enhanced performance over the original base design.

- **Energy Absorption Capability [EA]:** Energy absorption is a critical Key Performance Metric for fender samples, as it directly affects how well the fender protects marine vessels and docking structures from impact damage. When a vessel collides with a dock or another vessel, the fender must effectively absorb kinetic energy without transferring too much force to the vessel's hull. This capability minimizes the risk of damage to both the vessel and the docking infrastructure. Thus, energy absorption serves as a primary indicator of a fender's performance. The formula used to calculate this is as follows[46]:

$$EA = \int_0^d F ds \quad (3.5)$$

- **Specific Energy Absorption [SEA]:** Specific energy absorption is an essential performance metric for fender samples, as it provides an in-depth evaluation of the fender's effectiveness in absorbing impact energy relative to its mass. This measurement is vital because it not only reflects the total energy a fender can absorb but also emphasizes its efficiency in doing so, facilitating comparisons across different designs. A high specific energy absorption value indicates that the fender can protect vessels and docks effectively while potentially being lighter or using less material, leading to cost savings and easier handling or installation. This efficiency is especially crucial in scenarios where weight and space are limited, as it ensures optimal performance without adding unnecessary bulk. The calculation is based on the following formula[46]:

$$SEA = EA/m \quad (3.6)$$

- **Volume Fraction:** Volume fraction, defined as the ratio of the original fender sample's volume to that of the test fender sample, is a significant key performance metrics for fender design. This metric provides insight into the material efficiency used in the fender production. A well-optimized volume fraction indicates that the fender design uses the appropriate amount of material to achieve desired performance characteristics, such as energy absorption. This efficiency can lead to cost savings in material usage and manufacturing.

$$Vol_{frac} = Vol_{base}/Vol_{sample} \quad (3.7)$$

Ideally,  $Vol_{frac} = 1$  or  $Vol_{frac} > 1$

- **Stress Distribution:** Stress distribution plays a vital role in the performance and reliability of structural designs, including fenders. It refers to how internal forces are distributed

within a material when subjected to impacts. Proper management of stress distribution is essential to ensure that no single area of the material experiences excessive force, which could result in deformation or failure. For fender design, achieving a uniform stress distribution enhances the product's capacity to absorb and dissipate energy, thereby increasing its durability and lifespan. Monitoring stress distribution requires careful examination of high-stress areas and evaluation of von Mises stress values, which indicate a material's potential to yield. This analysis is critical for determining whether the material can endure the applied loads without failure. By comparing von Mises stress values to the material's Young's modulus, one can evaluate compliance with the von Mises yield criterion, which predicts the likelihood of material deformation or stability under load. This comparison is essential for ensuring that the design remains within safe limits, thus preventing material failure and improving overall structural integrity.

# 4

## Results

### 4.1. Results of the base fender

The impact scenario results for the base fender are essential, as they serve as the benchmark for comparing all other tested samples. This foundational data provides a reference point against which the performance improvements or deficiencies of other fender designs can be evaluated. Understanding how the base fender absorbs energy, deforms, and withstands impacts allows to assess the benefits of the design modifications made to alternative samples. Thus, the base fender's results form the cornerstone of the performance evaluation process, guiding the development and optimization of more effective fender solutions.

The forces that the fender might experience at various impact angles were obtained from ANSYS Workbench, providing crucial data for later testing of key performance parameters.

<b><i>Angles [ ° ]</i></b>	<b><i>Corresponding Velocities [mm/s]</i></b>	<b><i>Corresponding forces in N</i></b>
30	1286.11	6.3095
45	1818.83	12.626
60	2383.49	20.291
75	2484.57	21.177
90	2572.22	22.697

**Table 4.1:** Table displaying forces obtained from ANSYS Workbench corresponding to the various impact angles and velocities

As the impact angles rise from 30° to 90°, leading to increased impact velocities, both the reaction force and deformation magnitudes generally increase.

The base fender experienced a maximum deformation of  $23.786mm$  at the velocity  $2572.22mm/s$  indicating substantial material displacement during these more severe impacts.

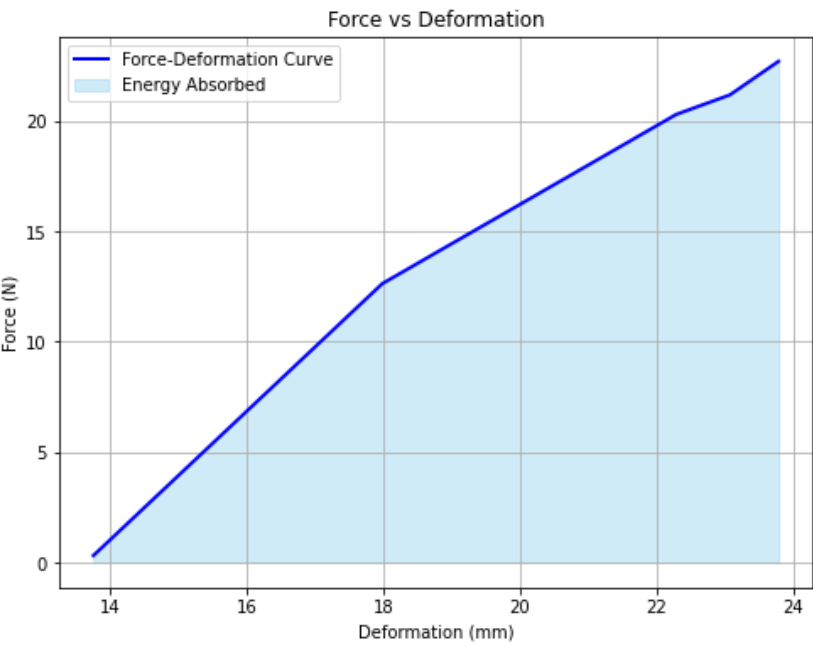


**Figure 4.1:** Figure showing Force vs Deformation graph of the Base Fender

In figure 4.1, the shaded area represents the energy absorbed by the fender during deformation, calculated as the area under the force-deformation curve. The energy absorption calculated for the base model sample is  $0.1334J$ .

	<i>EA</i>	<i>SEA</i>	<i>Volume</i>	<i>Maximum Equivalent Stress</i>
<i>Base Model</i>	0.1334J	0.7278 J/kg	$1.3692 * 10^5 mm^3$	0.3006 MPa

**Table 4.2:** Table presenting the key performance parameters of the base fender, which will serve as a benchmark for comparing the hybrid design samples

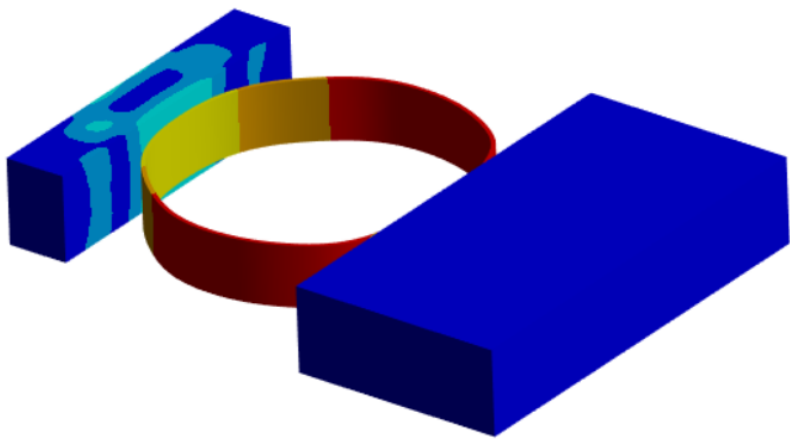


**Figure 4.2:** Figure illustrating the stress transferred to the boat body

Furthermore, it was observed that a maximum stress of  $9.1058 * 10^{-2}MPa$  was transferred to the body of the boat as shown in Figure 4.2. This is an important parameter to monitor to



determine if the hybrid samples transfer less stress to the boat body.

## 4.2. Dual-Method Energy Absorption

In the study of dual-method energy absorption mechanisms, the performance of traditional inflatable fenders was compared with a new hybrid design that integrates a lattice structure with honeycomb geometry.

Traditional inflatable fenders rely on pressurized air to provide cushioning and energy absorption through elastic deformation. These fenders are popular due to their simplicity and ease of deployment but have limitations in energy absorption capacity due to their reliance solely on air pressure.

The innovative hybrid design incorporating a lattice structure with honeycomb geometry demonstrated enhanced energy absorption properties. The honeycomb configuration allows for efficient distribution and dissipation of stress across the structure, significantly improving its ability to absorb and withstand impacts. Testing showed that this combination of the lattice structure with pressurized air led to considerable improvement in energy absorption capabilities compared to conventional designs.

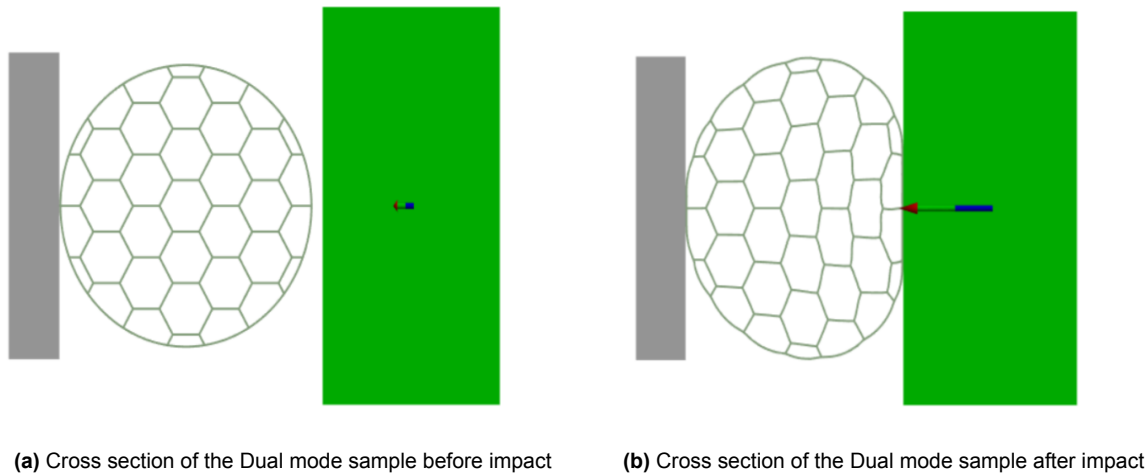


**Figure 4.3:** Figure depicting the impact of the dual-mode model

	<i>EA</i>	<i>Sample Mass</i>	<i>SEA</i>	<i>Volume Fraction</i>	<i>Max Stress</i>
<b>Dual Mode Sample</b>	0.9298J	0.37352kg	2.4892J/kg	0.4893	0.48114MPa

**Table 4.3:** Table showing the results of the hybrid dual-method sample

The findings suggest that incorporating a lattice honeycomb structure into inflatable fenders introduces a dual-method for energy absorption. This design leverages both the elasticity of pressurized air and the mechanical resilience and deformation behavior of the honeycomb structure, significantly improving the fender's ability to absorb impact energy. Under impact, the honeycomb structure offers extra support and a greater surface area than traditional fenders, enabling more efficient load distribution. This leads to a more controlled collapse, unlike standard air-filled fenders.

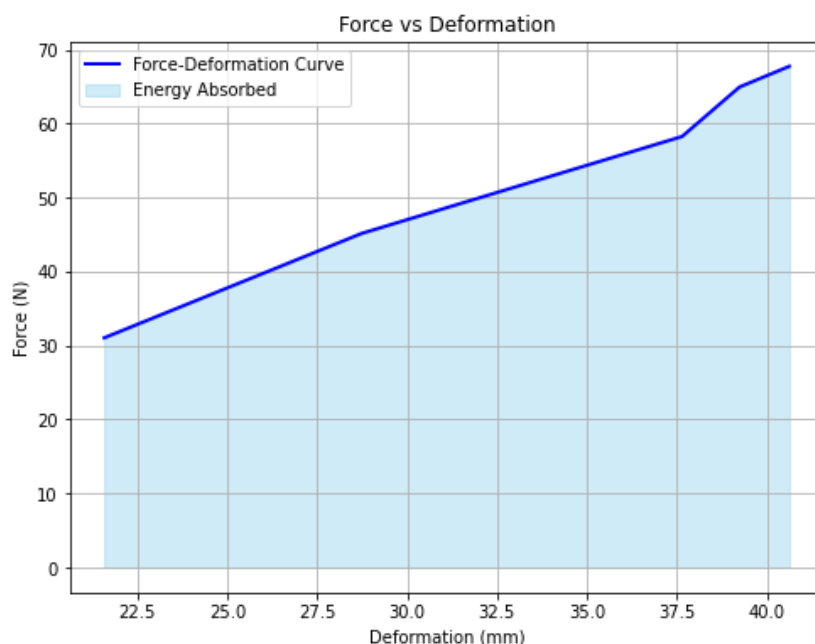


**Figure 4.4:** Figure illustrating the Force vs. Deformation graph for a fender incorporating honeycomb structures and filled with pressurized air

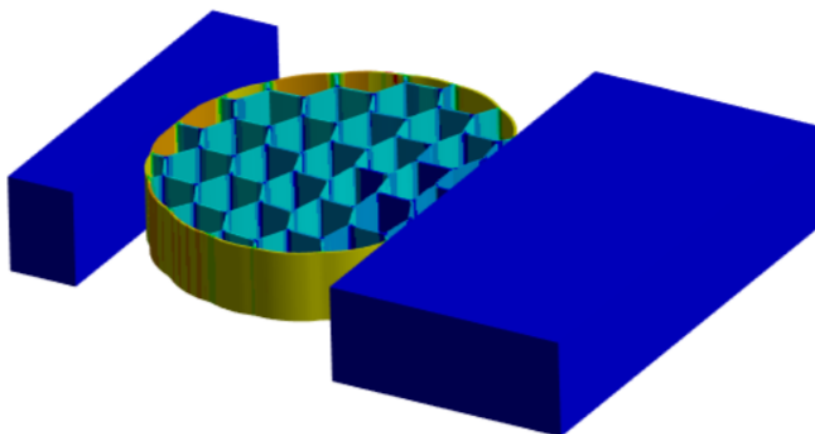


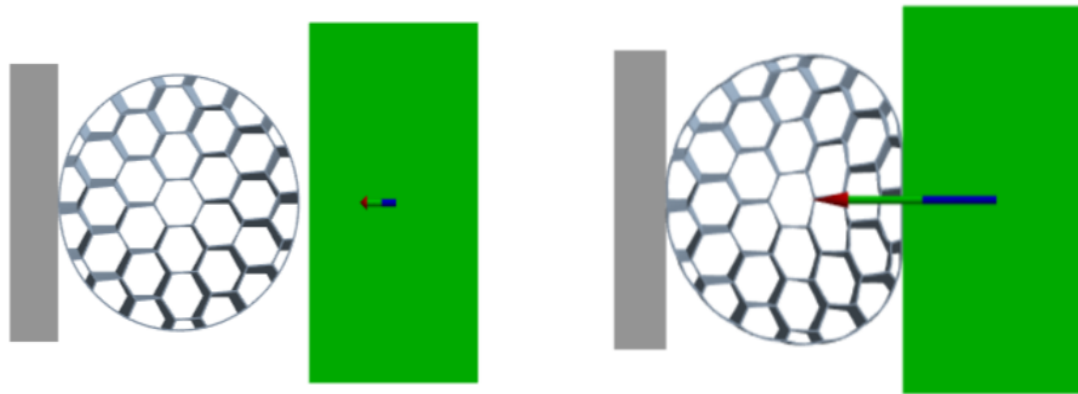
**Figure 4.5:** Figure illustrating the stress transferred to the boat body when using the dual-mode hybrid fender.

An important observation is that the stress transferred to the boat body is negligible, marking a significant improvement since the primary purpose of a fender is to minimize the stress and force transferred to the boat's hull. Additionally, the honeycomb structures within help ensure a more uniform distribution of stress as seen in Figure 4.5.

### 4.3. Enhanced Dual-Method Energy Absorption

The study of Enhanced Dual Method energy absorption compared the performance of traditional inflatable fenders with a new hybrid design that incorporates a lattice structure with honeycomb geometry. This new design is further improved by a unique twisting feature, inspired by the keratin lamellae in pangolin scales and eland horns (as detailed in 2.4). The introduction of twisting within the honeycomb structure allows for additional energy dissipation by adding a rotational deformation component. This mechanical transformation enhances the

system's overall energy absorption capabilities.



(a) Cross section of the Enhanced Dual Method with 5 deg twist before impact (b) Cross section of the Enhanced Dual Method with 5° twist after impact

**Figure 4.6:** Figure illustrating the first sample of the enhanced dual-method system.

Figure 4.6 displays the enhanced dual-method system, featuring honeycomb structures with a 5° twist, shown both before and after impact.

Additionally, Figure 4.7 presents the Force vs. Deformation curves for the fender samples with twisted honeycomb structures, where the twist angles range from 5° to 40°. The area under the Force vs. Deformation graph represents the energy absorbed. In most of the graphs, deformation increases with rising force. However, the sample with the 30° twisted honeycomb structure shows a distinct pattern: it initially follows a linear relationship between force and deformation, then levels off before rising again with a gentler slope.

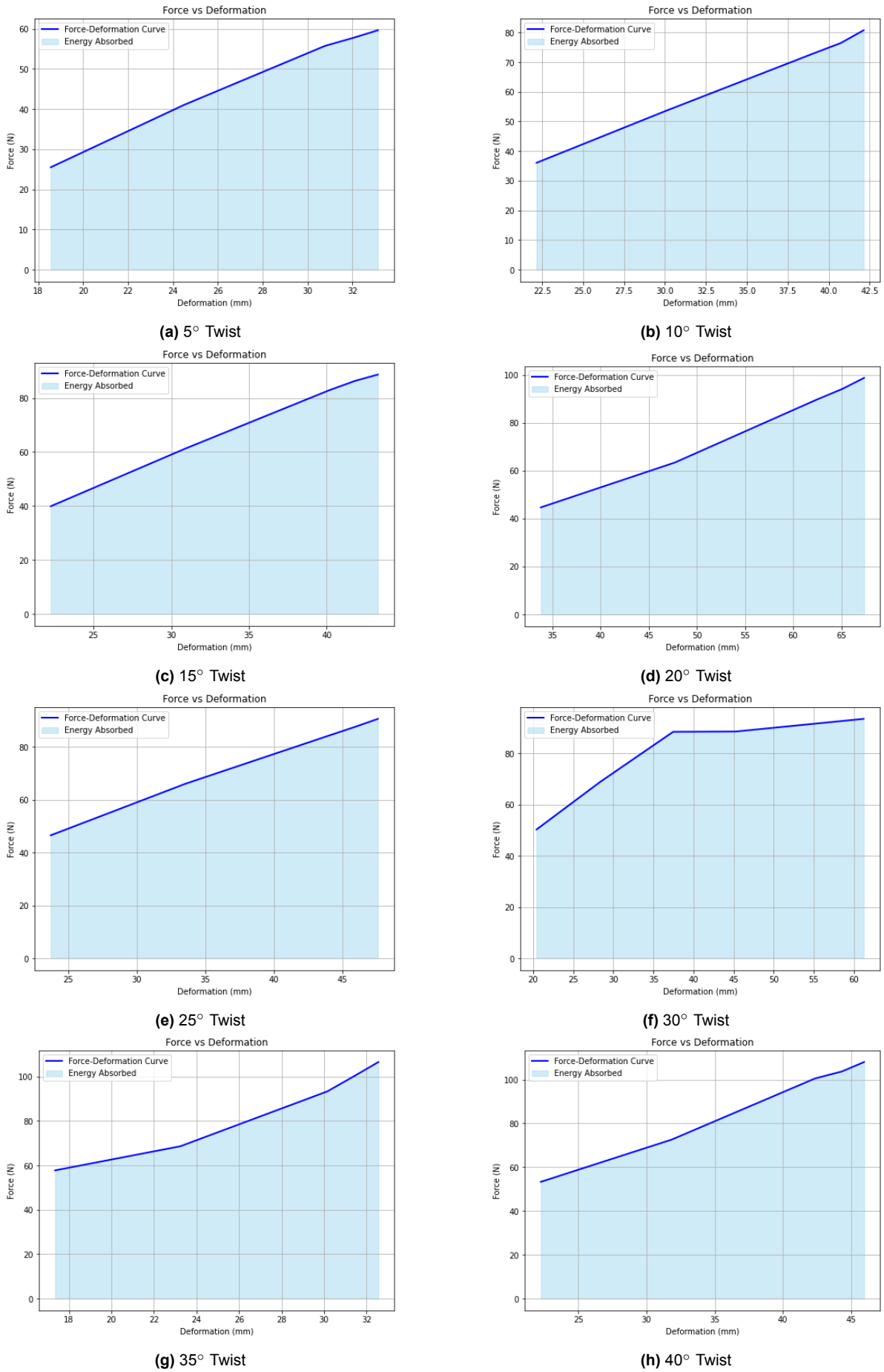


**Figure 4.7:** Figure illustrating the Force vs. Deformation graph for a fender incorporating twisted honeycomb structures and filled with pressurized air

Further, Figures 4.8 and 4.10 illustrate the samples with 20° and 30° twists, respectively, both before and after impact.

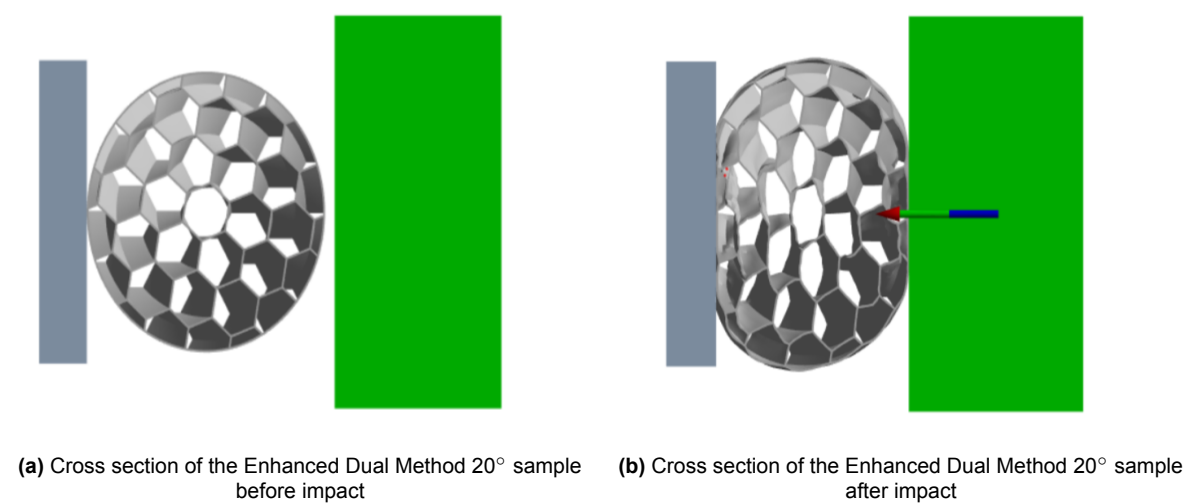


**Figure 4.8:** Figure depicting the impact of the Enhanced Dual Method System with 20° twist

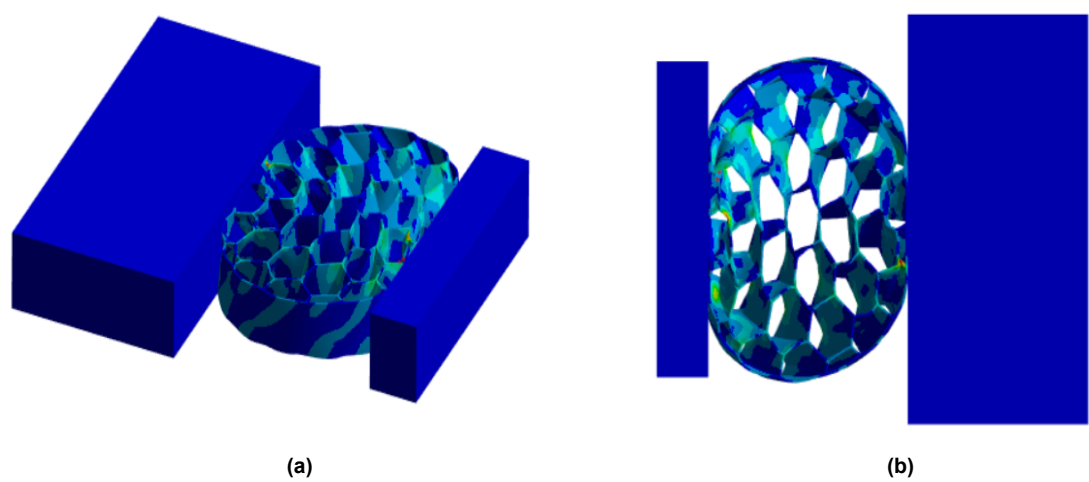
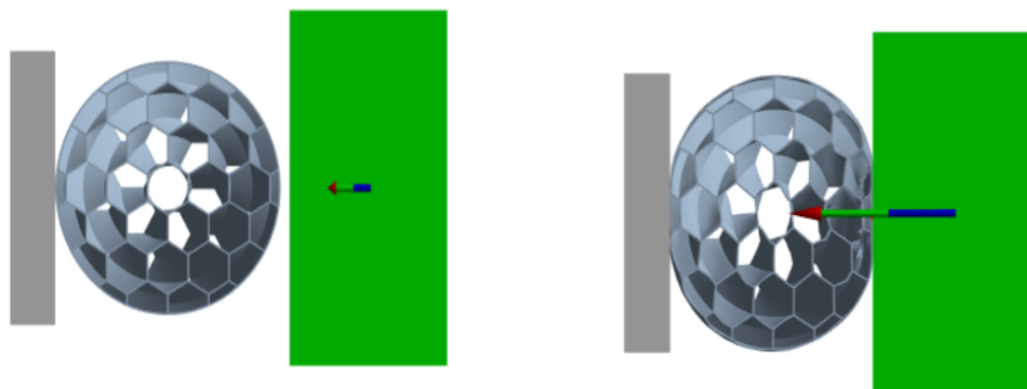


**Figure 4.9:** Figure depicting stress distribution of the enhanced dual method 20° twist model



(a) Cross section of the enhanced dual method 30° sample before impact

(b) Cross section of the enhanced dual 30° after before impact

**Figure 4.10:** Figure depicting the impact of the enhanced dual method 30° twist model

The quantitative values for the key performance metrics, as discussed in 3.3, were obtained from the simulations run for each sample and are presented in Table 4.4. As shown in Table 4.4, the highest energy absorption is observed at a 30° twist, with a value of 3.3241 J, followed by the 20° twist sample, which absorbed 2.3252 J. A similar trend is seen for specific energy absorption, as it is directly proportional to the energy absorbed relative to the sample's mass. It is also observed from the table that the maximum stress across all samples adheres to the von Mises stress criterion, as the stress values remain significantly lower than the material's Young's modulus.

	<i><b>EA</b></i>	<i><b>SEA</b></i>	<i><b>Volume Fraction</b></i>	<i><b>Max Stress</b></i>
<i><b>Base Fender</b></i>	0.1334 J	0.7278 J/kg	1	0.3006 MPa
<b>5°</b>	0.6388 J	1.6488 J/kg	0.4718	0.48859 MPa
<b>10°</b>	1.1590 J	3.0170 J/kg	0.4758	0.74833 MPa
<b>15°</b>	1.3762 J	3.6429 J/kg	0.4838	1.2758 MPa
<b>20°</b>	2.3252 J	6.1357 J/kg	0.4823	2.4668 MPa
<b>25°</b>	1.6585 J	4.4752 J/kg	0.4932	1.9658 MPa
<b>30°</b>	3.3241 J	9.0272 J/kg	0.4964	1.5039 MPa
<b>35°</b>	1.1601 J	3.1252 J/kg	0.4924	2.241 MPa
<b>40°</b>	1.8765 J	5.0302 J/kg	0.4899	2.9961 MPa

**Table 4.4:** Table showing the results of the hybrid Triple-Mode sample

Finally, Figures 4.11 and C.6 illustrate the variations in Energy Absorption and Specific Energy Absorption as the twist angle increases from 5° to 40°. The graphs indicate the presence of a distinct global maximum, along with several local maxima.

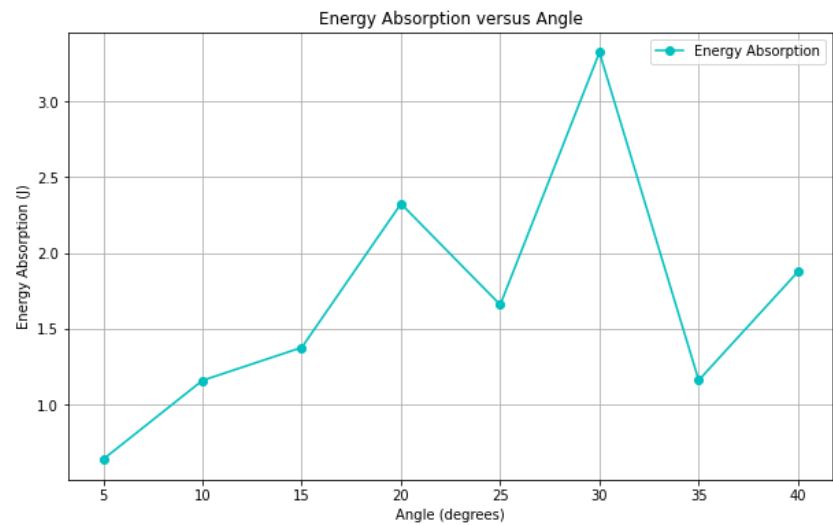


**Figure 4.11:** Figure showing Energy Absorption Fluctuations from 5° to 40° Twist

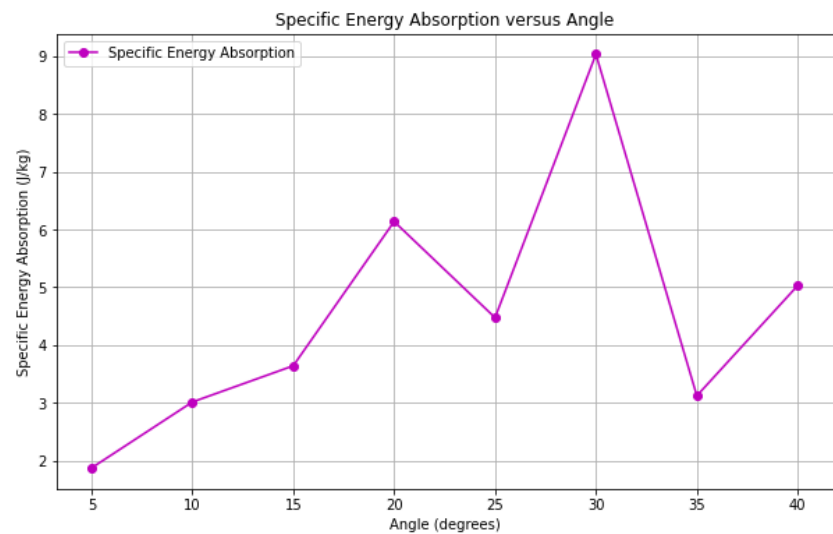


**Figure 4.12:** Figure showing Specific Energy Absorption Fluctuations from 5° to 40° Twist

# 5

## Discussions

### 5.1. Interpretation of the results of the twisted structures

The experiments initially applied a  $5^\circ$  twist to the honeycomb lattice structure, but this setup failed to enhance energy absorption and actually performed worse than the dual-method system without twisting. This lack of improvement can likely be attributed to a structural activation threshold, as the minimal  $5^\circ$  twist did not activate the mechanism's full capabilities. It's probable that the geometry of the honeycomb lattice requires a larger angle to effectively redistribute stress and utilize the structural transformation properties intended to boost energy absorption. Notably, the  $5^\circ$  twist resulted in reduced energy absorption, with the energy absorption (EA) at  $0^\circ$  (Dual Method) being approximately 0.98 Joules shown in Table 4.4, compared to only 0.63 Joules in the sample twisted at  $5^\circ$ . Performance improvements were observed only when the twisting angle was increased beyond the initial  $5^\circ$ , highlighting the importance of optimizing angular deformation to achieve effective energy dissipation.

Further, energy absorption increases with the angle of twist in honeycombs from  $10^\circ$  to  $20^\circ$  as seen in figure 4.11. Up to  $20^\circ$ , the twisting deformation leads to a more efficient compaction of the honeycomb structures and air pockets, maximizing energy absorption due to synergies between compression and torsional forces. This may result in an optimal configuration where both the structure of the fender and its internal components, that's the honeycomb, work together efficiently. Beyond  $20^\circ$ , as the twist angle increases, certain cells within the honeycomb undergo localized buckling, which results in less uniform deformation and, consequently, varying efficiency in energy absorption throughout the structure. This phenomenon contributes to the fluctuations in energy absorption observed at higher twist angles.

The critical angle of  $20^\circ$  represents a pivotal point in the deformation behavior of the honeycomb structures within the fender, where energy absorption reaches its peak efficiency. This optimal functionality can be attributed to the interplay between elastic and torsional deformation modes, which provide a synergistic enhancement to the fender's performance.

At this angle, the honeycomb structures undergo a significant elastic deformation, allowing them to store energy temporarily and release it once the stress is removed. This reversible deformation contributes to maintaining the structural integrity of the fender and prevents permanent deformations that could reduce its long-term effectiveness.

When the honeycomb cells are twisted by  $20^\circ$  around the center of the fender, a torsional deformation mode is introduced. This twisting motion generates stress across the structure,



aligning the internal forces to manage the imposed compressive loads more efficiently. The torsional deformation also increases the effective density of the honeycomb, enabling it to dissipate energy more effectively. By optimizing the interaction between torsional and compressive forces, the honeycomb structure enhances its energy-absorbing capacity and overall resilience under load.

Additionally, as seen in figure 4.9, the  $20^\circ$  twist alignment ensures that forces are evenly distributed throughout the fender, preventing localized stress concentrations. Twisting the honeycomb structures creates well-defined load pathways that allow for the even distribution of stresses. This means that any force exerted on the fender is effectively channeled through these pathways, reducing the likelihood of stress hotspots. The twist effectively interlocks the cells in a way that shares the mechanical load uniformly. By promoting a uniform stress field, the  $20^\circ$  twist mitigates the development of weak points that could arise from uneven force application or cellular misalignment. This homogeneity in stress distribution supports the prevention of material fatigue and potential areas of failure, enhancing the overall resilience of the fender.

The interplay between these deformation modes at the critical  $20^\circ$  angle allows the fender's internal honeycomb elements to function optimally. The twisting helps compact the honeycomb structures and internal air pockets, facilitating an efficient balance between torsional and elastic responses under compressive loading.

Conversely, while the  $30^\circ$  twist in the honeycomb structures within the fender achieves maximum energy absorption, specific observations from simulations highlight potential limitations of this design. This structure, demonstrates an initial linear force vs. deformation relationship, transitioning to a plateau (horizontal line) and then back to a linear regime with a reduced slope as seen in Figure 4.7 (f). This indicates that the structure has entered a phase where further deformation occurs at a relatively constant force. This suggests that the material is approaching its energy absorption limit. While desirable for absorbing sustained impacts, this behavior also signals limited capacity for further energy absorption, risking structural compromise if additional or unexpected loads occur.

Further, figure 4.10b shows that not the entire  $30^\circ$  twisted honeycomb structure compresses. Instead, only the cells around the circumference where the impact occurs experience significant crushing. This non-uniform deformation suggests that the twist may inhibit full structural engagement, which could limit the fender's ability to distribute impact forces evenly throughout the structure.

While enhanced energy absorption at the  $30^\circ$  twist suggests effective initial performance, the downsides, including increased stiffness, plateaued force-displacement, and uneven compression, indicate a trade-off between absorption efficiency and structural flexibility.

## 5.2. Limitations

This study, while offering critical insights into enhancing maritime fender performance with honeycomb lattice structures, encountered several limitations. Notably, only a  $50mm$  thick sample of the fender was tested rather than the entire fender. This choice simplifies the analysis but may not fully capture the behavior of the full-scale fender under similar conditions. As such, extrapolating the results to predict the performance of the entire fender could introduce inaccuracies, making further investigation essential.

One notable limitation of this study is that the simulations and analyses were conducted using a vessel impact velocity of  $5kn$ , intended to represent a worst-case scenario for impact forces

during docking events. While useful for establishing a benchmark for the fender's protective capabilities, this velocity may not accurately reflect typical operational conditions across all maritime scenarios. In reality, docking velocities can vary significantly based on vessel type, environmental conditions, and port regulations.

One of the critical limitations of this study is the consideration of velocity components derived from a  $5kn$  speed with corresponding magnitudes calculated at angles of  $30^\circ$ ,  $45^\circ$ ,  $60^\circ$ ,  $75^\circ$ , and  $90^\circ$ . While this approach allowed for varying force values from the simulation to assess energy absorption, the impact force on the fender was always applied normal to the structure, simulating a  $90^\circ$  impact. In reality, impact forces during docking can occur from multiple directions and not just perpendicularly, substantially influencing how a fender responds to such forces. This simplification in the simulation setup may not accurately represent the complex interactions in a real docking scenario, potentially affecting the reliability of the conclusions drawn regarding the fender's performance.

Additionally, the assumption of a constant air temperature inside the fender was made for modeling simplicity. This assumption does not fully account for potential fluctuations in air temperature that could influence material behavior and energy absorption capabilities. Furthermore, environmental factors such as humidity and salinity were not considered, which might affect the fender's durability and effectiveness over time.

Further, volume ratio is for the sample with  $20^\circ$  twist is around 0.4823. A larger volume of the proposed design suggests more material is used in the new model, which could impact the cost of production and overall manufacturing expenses.

Lastly, another one of the limitations of this study is the increased mass of the new fender design compared to the base fender sample. While the integration of honeycomb lattice structures significantly enhances energy absorption capabilities, this design inherently adds weight to the fender. For boats, heavier fenders present difficulties in terms of handling, making them less convenient for the crew to deploy, retrieve, and store, especially during docking when quick adjustments are essential. Their increased weight can cause added physical strain on crew members, potentially requiring more personnel or mechanical tools to manage them. Additionally, their bulkiness may take up valuable storage space on the boat and affect the vessel's performance due to the added weight. These challenges can decrease efficiency and make fender management more labor-intensive during critical operations.

### 5.3. Future Work

For future research efforts, the initial step involves enhancing simulation models to incorporate multi-directional impact scenarios. This will better capture the diverse response behaviors of fenders under realistic docking conditions and provide a more accurate assessment of their performance.

Further, an important next step would involve extrapolating the simulation results to the entire fender structure. This process would provide a more comprehensive understanding of the fender's behavior under varying loads and deformations. Once the simulation results for the full structure are obtained, they should be compared with the berthing energy equations outlined in Section B. This comparison would help validate the accuracy of the simulations and ensure that the model effectively captures the energy absorption characteristics predicted by theoretical equations. By aligning these results, we can refine the model for enhanced predictive capabilities and performance optimization.

After refining the simulation, the next crucial step is to fabricate a prototype for thorough test-

ing under real-world conditions. This testing will allow for the evaluation of the fender's performance and provide insights into any discrepancies between the simulation predictions and actual behavior. Identifying such differences will offer valuable opportunities to further refine both the model and the overall design approach, ensuring the final product performs as expected in practical applications.

Subsequently, conducting fatigue analysis is essential to assess the long-term viability and resilience of the fender design under cyclic loading conditions. Comparing results from the base fender and the enhanced 20° model will provide further insights into the effectiveness of design modifications.

Lastly, exploring alternative materials to PVC for the recommended design could offer significant benefits in terms of performance, durability, and sustainability. Materials such as thermoplastic elastomers, rubber composites, or advanced polymers may provide improved energy absorption, resistance to environmental factors, and enhanced lifespan under repeated stress. Additionally, materials with higher recyclability or lower environmental impact could align with sustainability goals. Conducting material testing and simulations on these alternatives would help identify the most suitable options for optimizing the fender's performance while addressing potential limitations of PVC.

# 6

## Conclusion

This thesis investigated the innovative enhancement of traditional air-filled boat fenders by incorporating honeycomb lattice structures to significantly improve energy absorption while retaining PVC as the base material. The research focused on optimizing energy dissipation and improving reliability through structural design.

The study introduced alternative configurations, particularly honeycomb structures, which were modeled to assess their potential for optimizing energy absorption. The hybrid design, combining air-filled chambers with honeycomb structures, demonstrated superior performance under controlled conditions compared to traditional PVC fenders. The comparative analysis showed that the honeycomb-enhanced fenders provided greater durability and energy absorption, contributing to the overall resilience of the fender system.

One key finding was the identification of a structural activation threshold at approximately  $10^\circ$  of twist, at which the honeycomb structures begin to engage efficiently in energy absorption. Below this threshold, particularly at  $5^\circ$  of twist, performance was less effective due to insufficient structural engagement and load distribution. As the twist angle increased, energy absorption improved steadily up to  $20^\circ$ , after which performance began to fluctuate. This fluctuation is attributed to localized buckling in the honeycomb cells at higher twist angles, which led to uneven deformation and reduced energy absorption efficiency.

The research identified  $20^\circ$  of twist as the optimal angle for maximizing energy absorption. At this angle, the honeycomb structures achieved uniform stress distribution and full engagement without introducing excessive stiffness. However, at  $30^\circ$  of twist, although energy absorption initially increased, the added stiffness caused uneven compression and limited the fender's ability to distribute stress effectively. This resulted in a plateau in the force-displacement curve, highlighting potential design inefficiencies at higher twist angles.

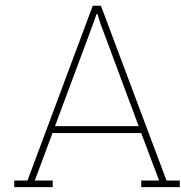
Ultimately, the findings emphasize the importance of balancing twist angles to optimize structural flexibility and energy management. By addressing the research questions, this study confirmed that honeycomb lattice structures significantly enhance energy absorption compared to traditional air-filled PVC fenders, and design optimization—specifically through twisting mechanisms—plays a critical role in maximizing performance.

# References

- [1] Wojciech Koziół and Wiesław Galor. “Some problems of berthing of ships with non-conventional propulsions”. In: *TransNav, International Journal on Marine Navigation and Safety of Sea Transportation* 1.3 (2007), pp. 319–323.
- [2] Jerry Thermos. *Choosing the Right Marine Fenders*. 2024. URL: <https://www.marinefendersintl.com/choosing-marine-fenders/> (visited on 03/20/2024).
- [3] LTD CHONGQING YUSHUO CO. *Comparative Analysis of Rubber Fenders vs. Foam-filled Fenders*. 2024. URL: <https://www.ysmarines.com/articles/comparative-analysis-of-rubber-fenders-and-foam-filled-fenders/#1-energy-absorption> (visited on 07/2022).
- [4] Thomas E Spencer. “Marine fender systems”. In: *Ports 2004: Port Development in the Changing World*. 2004, pp. 1–10.
- [5] Houcine Zniker et al. “Energy absorption and damage characterization of GFRP laminated and PVC-foam sandwich composites under repeated impacts with reduced energies and quasi-static indentation”. In: *Case studies in construction materials* 16 (2022), e00844.
- [6] John Magliaro et al. “Influence of Extruded Tubing and Foam-Filler Material Pairing on the Energy Absorption of Composite AA6061/PVC Structures”. In: *Materials* 16.18 (2023), p. 6282.
- [7] Aleix Escorsell. *How many fenders do I need for my boat? - A complete guide*. 2022. URL: <https://www.sail-world.com/news/252339/How-many-fenders-do-I-need-for-my-boat> (visited on 10/04/2022).
- [8] Armin Yousefi et al. “3D-Printed Soft and Hard Meta-Structures with Supreme Energy Absorption and Dissipation Capacities in Cyclic Loading Conditions”. In: *Advanced Engineering Materials* 25.4 (2023), p. 2201189.
- [9] Mahdi Bodaghi et al. “Metamaterial boat fenders with supreme shape recovery and energy absorption/dissipation via FFF 4D printing”. In: *Smart Materials and Structures* 32.9 (2023), p. 095028.
- [10] Prof. Dr.-Ing. habil. Carolin Körner. *Cellular mechanical metamaterials*. 2022. URL: <https://www.wtm.tf.fau.eu/forschung/additive-fertigung/cellular-mechanical-metamaterials/> (visited on 10/04/2022).
- [11] The European Council of Vinyl Manufacturers. *PVC’s physical properties*. 2024. URL: <https://pvc.org/about-pvc/pvcs-physical-properties/> (visited on 12/2023).
- [12] Ltd. Team Rapid MFG Co. *PVC Plastic : Properties, manufacturing, Types, Processes, and Uses*. 2024. URL: <https://www.team-mfg.com/blog/pvc-plastic.html>.
- [13] Heong Jin Kim et al. “SOLID RUBBER FENDERS TO PREVENT STRUCTURAL DAMAGE IN A LOWSPEED COLLISION BETWEEN A SHIP-SHAPED OFFSHORE INSTALLATION AND A SHUTTLE TANKER WORKING SIDE-BY-SIDE IN OFFLOADING OPERATION.” In: *International Journal of Maritime Engineering-Transactions of the Royal Institute of Naval Architects-Part A* 165 (2023).

- [14] Shigeru Ueda et al. "Reliability design method of fender for berthing ship". In: *International Navigation Congress (30th: 2002: Sydney, NSW)*. Institution of Engineers Sydney, NSW. 2002, pp. 692–707.
- [15] Joanna Tuleja et al. "Evaluation of the Possibility of Increasing the Energy Absorption Efficiency of Fender Devices Using the Example of Cylindrical Fenders with Additional Structural Elements Applied". In: *Energies* 16.3 (2023), p. 1165.
- [16] Mahmud Shahriare Atiq, AK Shajib, et al. "Analysis of Marine Fender Systems Minimizing the Impact of Collision Damage". In: *Proceedings of the 13th International Conference on Marine Technology (MARTEC 2022)*. 2023.
- [17] Alfred Roubos et al. "Partial safety factors for berthing velocity and loads on marine structures". In: *Marine structures* 58 (2018), pp. 73–91.
- [18] Shigeki Sakakibara and Masayoshi Kubo. "Ship berthing and mooring monitoring system by pneumatic-type fenders". In: *Ocean engineering* 34.8-9 (2007), pp. 1174–1181.
- [19] Captain Bob Gilchrist. *THE IMPORTANCE OF PNEUMATIC FENDERS FOR SHIP-TO-SHIP TRANSFERS: A SERVICE PROVIDER'S PERSPECTIVE*. 2024. URL: <https://www.safests.com/wp-content/uploads/2021/03/Fender-Position-Paper.pdf>.
- [20] W. Johnson and S. R. Reid. "METALLIC ENERGY DISSIPATING SYSTEMS." English. In: *Applied Mechanics Reviews* 31.3 (Jan. 1978), pp. 277–288. ISSN: 0003-6900.
- [21] W Johnson. "The elements of crashworthiness: scope and actuality". In: *Proceedings of the Institution of Mechanical Engineers, Part D: Journal of Automobile Engineering* 204.4 (1990), pp. 255–273.
- [22] Guoxing Lu and TX Yu. *Energy absorption of structures and materials*. Elsevier, 2003.
- [23] EW Andrews, Lorna J Gibson, and MF Ashby. "The creep of cellular solids". In: *Acta materialia* 47.10 (1999), pp. 2853–2863.
- [24] Lily Trestan et al. "Mechanical Analysis of Animal Horns". In: ().
- [25] Jamil Cappelli et al. "The bony horncore of the common eland (*Taurotragus oryx*): composition and mechanical properties of a spiral fighting structure". In: *Journal of Anatomy* 232.1 (2018), pp. 72–79.
- [26] Mike Briggs and Peggy Briggs. *The encyclopedia of world wildlife*. Parragon Publishing India, 2006.
- [27] Yasuaki Seki et al. "The toucan beak: structure and mechanical response". In: *Materials Science and Engineering: C* 26.8 (2006), pp. 1412–1420.
- [28] Luca Tombolato et al. "Microstructure, elastic properties and deformation mechanisms of horn keratin". In: *Acta biomaterialia* 6.2 (2010), pp. 319–330.
- [29] Gerald Cubitt; Anita Mishra; Elsa Bussiere. *What is a pangolin?* 2022. URL: <https://www.savepangolins.org/what-is-a-pangolin> (visited on 2022).
- [30] Zengqian Liu et al. "Functional gradients and heterogeneities in biological materials: Design principles, functions, and bioinspired applications". In: *Progress in Materials Science* 88 (2017), pp. 467–498.
- [31] Bin Wang et al. "Pangolin armor: overlapping, structure, and mechanical properties of the keratinous scales". In: *Acta biomaterialia* 41 (2016), pp. 60–74.
- [32] Thomas C Hales. "The honeycomb conjecture". In: *Discrete & computational geometry* 25 (2001), pp. 1–22.

- [33] Chang Qi, Feng Jiang, and Shu Yang. "Advanced honeycomb designs for improving mechanical properties: A review". In: *Composites Part B: Engineering* 227 (2021), p. 109393.
- [34] Haijun Yu et al. "Research into the effect of cell diameter of aluminum foam on its compressive and energy absorption properties". In: *Materials Science and Engineering: A* 454 (2007), pp. 542–546.
- [35] Sardar Malek and Lorna Gibson. "Effective elastic properties of periodic hexagonal honeycombs". In: *Mechanics of Materials* 91 (2015), pp. 226–240.
- [36] Jaeung Chung and Anthony M Waas. "Compressive response of circular cell polycarbonate honeycombs under inplane biaxial static and dynamic loading. Part I: experiments". In: *International journal of impact engineering* 27.7 (2002), pp. 729–754.
- [37] Lorna J Gibson. "Cellular solids". In: *Mrs Bulletin* 28.4 (2003), pp. 270–274.
- [38] Qiao Zhang and Hu Liu. "On the dynamic response of porous functionally graded microbeam under moving load". In: *International Journal of Engineering Science* 153 (2020), p. 103317.
- [39] Chao Quan et al. "3d printed continuous fiber reinforced composite auxetic honeycomb structures". In: *Composites Part B: Engineering* 187 (2020), p. 107858.
- [40] Alfred Roubos, Leon Groenewegen, and Dirk Jan Peters. "Berthing velocity of large seagoing vessels in the port of Rotterdam". In: *Marine Structures* 51 (2017), pp. 202–219.
- [41] Majoni. *SPORTDEAL*. 2024. URL: <https://www.sportdeal.nl/classic-cilinder-fenders-zwart-alle-matenc-8712256001039+size-10~x~42~cm> (visited on 10/2018).
- [42] Taylor-Made. *Fender Buoy: Inflation Instructions*. 2017. URL: [https://defender.com/assets/pdf/taylor-made/taylor\\_inflate.pdf](https://defender.com/assets/pdf/taylor-made/taylor_inflate.pdf) (visited on 2017).
- [43] Mohammad Esgandari and Oluremi Olatunbosun. "Implicit–explicit co-simulation of brake noise". In: *Finite Elements in Analysis and Design* 99 (2015), pp. 16–23.
- [44] Nickolay Y Gnedin, Vadim A Semenov, and Andrey V Kravtsov. "Enforcing the Courant–Friedrichs–Lewy condition in explicitly conservative local time stepping schemes". In: *Journal of Computational Physics* 359 (2018), pp. 93–105.
- [45] Richard Courant, Kurt Friedrichs, and Hans Lewy. "Über die partiellen Differenzengleichungen der mathematischen Physik". In: *Mathematische annalen* 100.1 (1928), pp. 32–74.
- [46] Shuguang Yao et al. "Energy absorption characteristics of square frustum lattice structure". In: *Composite Structures* 275 (2021), p. 114492.
- [47] Wiesław Galor. "The analysis of effective energy of ship's berthing to the quay". In: *Journal of KONES* 19 (2012), pp. 185–191.



# Calculation

## *Energy Absorption code*

```
1
2
3 import numpy as np
4 from scipy.integrate import simps
5 import matplotlib.pyplot as plt
6
7 # Prompt user to enter the force array in Newtons
8 force_input = input("Enter the force values in Newtons, separated by spaces:")
9 force = np.array([float(f) for f in force_input.split()])
10
11 # Prompt user to enter the deformation array in millimeters
12 deformation_input = input("Enter the deformation values in millimeters, separated by spaces:")
13 deformation = np.array([float(d) for d in deformation_input.split()])
14
15 # Check if the lengths of the arrays are the same
16 if len(force) != len(deformation):
17     print("Error: The force and deformation arrays must be of the same length.")
18 else:
19     # Calculate the energy absorption using the trapezoidal rule (simpson's method
20     # as an example)
21     # Convert deformation from millimeters to meters for energy calculation
22     deformation_meters = deformation / 1000.0
23     energy_absorbed = simps(force, x=deformation_meters)
24
25     # Print the energy absorbed
26     print(f"Energy Absorbed: {energy_absorbed} Joules")
27
28     # Plotting the force-deformation curve
29     plt.figure(figsize=(8, 6))
30     plt.plot(deformation, force, color='b', linewidth=2, label='Force-Deformation Curve')
31     plt.fill_between(deformation, force, color='skyblue', alpha=0.4, label='Energy Absorbed')
32     plt.title('Force vs Deformation')
33     plt.xlabel('Deformation (mm)')
34     plt.ylabel('Force (N)')
35     plt.legend()
36     plt.grid(True)
37     plt.show()
```



# B

## Energy Equations

The following equations are employed to calculate the berthing energy for a range of vessels, serving as a theoretical model for comparison with the extrapolated results. These equations provide a basis for evaluating the accuracy and consistency of the experimental data against established theoretical predictions [47].

$$E_B = \frac{1}{2} * W_D * v_B^2 * C_M * C_E * C_C * C_S$$

Where,

$W_D$  = Displacement of the vessel (kg)

$E_B$  is the kinetic energy of the boat

$v_B$  Realistic normal component of boats's velocity to the wharf ( $\frac{m}{s}$ )

$C_M$  is the Virtual mass coefficient, which accounts for the additional mass from entrained water, with typical values ranging from 1.3 to 1.8 and,

$$C_M = 1 + \frac{2 * D}{B}$$

Where, B is the Breadth of the boat and D is the Draft of the boat

$C_E$  is the Eccentricity coefficient, which is determined based on the rotation of a boat (e.g., angle of approach), with typical values ranging from 0.5 to 0.8 and,

$$C_E = \frac{K^2 + R^2 * \cos^2 \gamma}{K^2 + R^2}$$

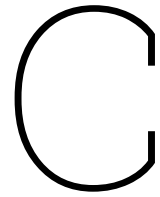
Where, K= Radius of gyration of the vessel (usually  $\frac{1}{4}$  the vessel's length)

R= Distance of the line parallel to the jetty measured from the ship's center of gravity to the point of contact, usually  $\frac{1}{5} - \frac{1}{4}$  of the ship's length

$$\gamma = 90^\circ - \alpha - \arcsin \frac{B}{2R}$$

$C_C$  is Configuration coefficient, which is defined by the geometry and type of the berth, with typical values ranging from 0.8 to 1

$C_S$  is Softness coefficient, which is derived to reflect the relative stiffness between the ship hull and the fender, with typical values ranging from 0.9 to 1



# Documentation of Experimental Observations and Rejected Design Concepts

A dynamic analysis was initially performed on basic lattice structures to assess their response characteristics. This examination aimed to understand how these structures behave under various conditions and loads.

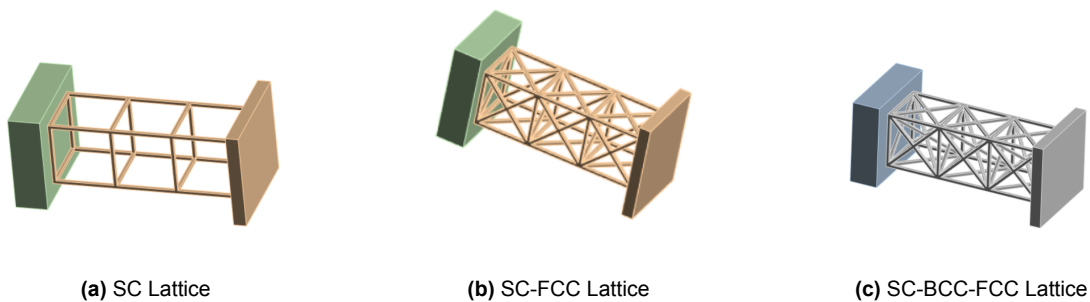


**Figure C.1:** Figure showing Impact Analysis of Lattice Structures

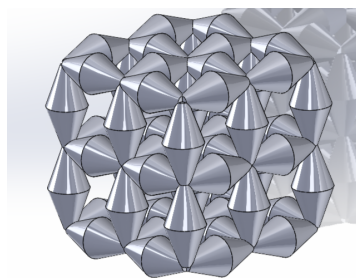
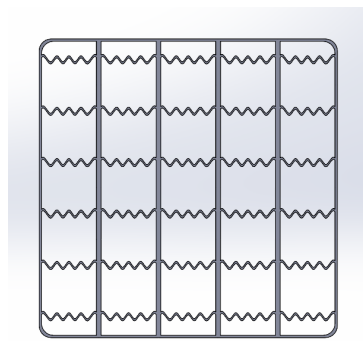
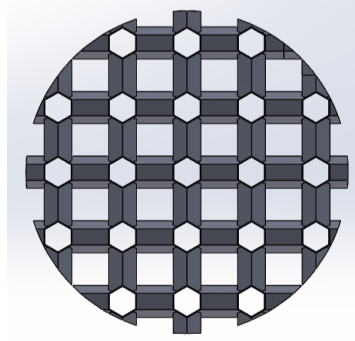


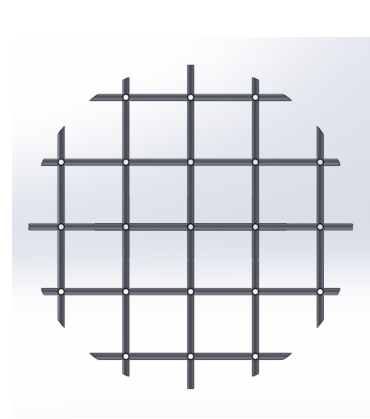
**Figure C.2**



(a) Figure of Square Cross-section  
Fender filled with unit cells inspired by  
cork cells

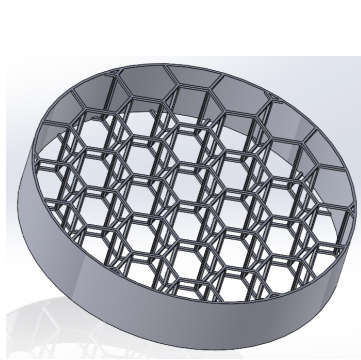


(b) Figure of Circular Cross-section  
Fender filled with unit cells with  
hexagon profile inspired by TPMS  
lattice

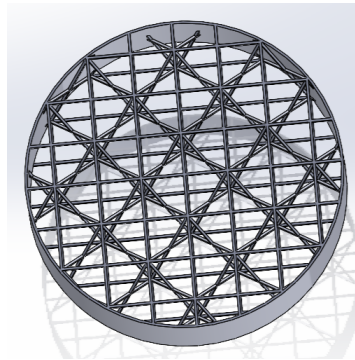


(c)

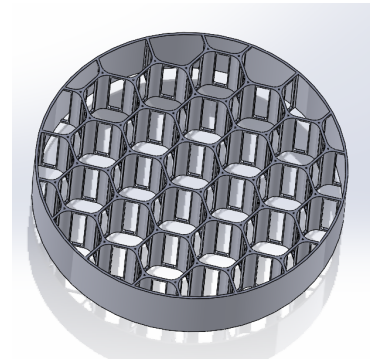
**Figure C.3: Rejected samples 1**



(a)

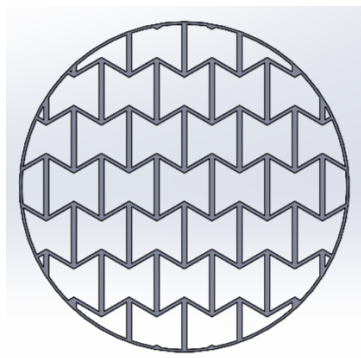


(b)

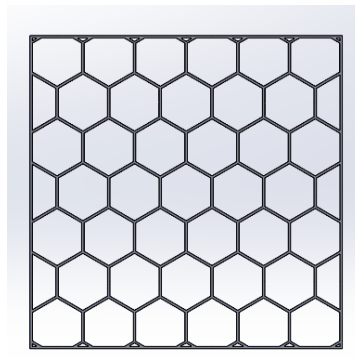


(c)

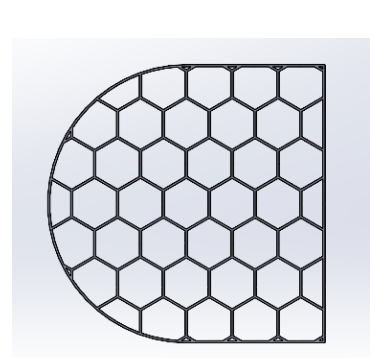
**Figure C.4: Rejected samples 2**



(a)



(b)



(c)

**Figure C.5: Rejected samples 3**

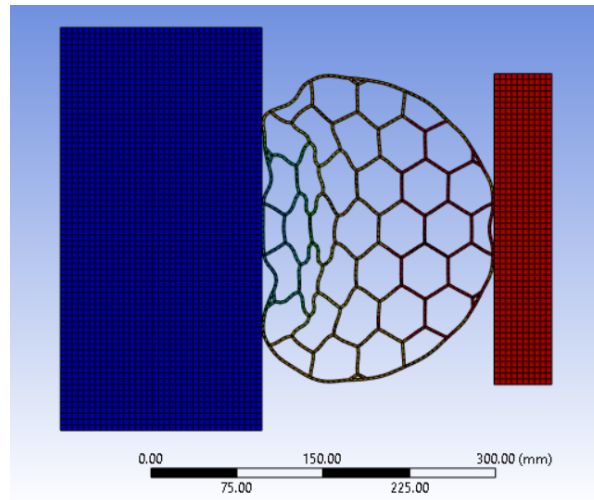


**Figure C.6:** PVC Fender without Air

## C.1. Monitoring and Analysis of Energy Metrics

Monitoring of energy metrics was critical for evaluating structural performance and energy management. This process involved detailed scrutiny of energy conservation and energy summary graphs, which provided insights into the dynamic behavior of the fender models under various impact and deformation scenarios.

- **Energy Conservation Tracking:** Throughout each simulation, the total energy of the system was closely monitored to ensure that no artificial energy gains or losses occurred, which could undermine the validity of the results. By confirming that the total energy remained constant, we validated the stability and accuracy of the model setups.
- **Kinetic and Internal Energy Transformation:** The transformation from kinetic to internal energy was a focal point of analysis, reflecting how effectively the fender absorbed and dissipated impact energy. Critical attention was given to ensure that increases in internal energy corresponded with expected deformation modes under compressive loads.
- **External Work and Contact Energy:** In simulations involving direct impacts and dynamic interactions, the external work and contact energy metrics were examined to understand how applied loads were being transferred into the fender structure. This was particularly relevant for assessing the efficiency of energy transfer and the effectiveness of the honeycomb configurations.
- **Energy Error Monitoring:** A crucial aspect of the analysis involved monitoring the energy error throughout the simulations. Special attention was given to detect any rapid increases in energy error, which could indicate numerical instability within a few cycles of the solution process. If the energy error rose quickly, it signaled potential inaccuracies in the simulation, necessitating adjustments to the model parameters, mesh refinement, or timestep settings to maintain solution integrity.

## C.2. Rationale for Circular Cross-Section

The decision to use a circular cross-section for the fender, filled with honeycomb unit cells, was based on several considerations. A circular cross-section allows for more even stress distribution and minimizes stress concentrations, especially critical in high-impact scenarios. This geometry enhances energy absorption and dissipation due to its ability to uniformly distribute

forces across the fender. The inherent radial symmetry of a circular shape also provides resistance against torsional and bending stresses, complementing the benefits of the honeycomb structure's energy absorption capabilities.

In contrast, a square cross-section could lead to stress concentration at the corners, potentially compromising the fender's durability and energy absorption efficiency. Thus, the circular design optimizes the fender's ability to handle physical forces encountered during docking and berthing, reducing the risk of structural failure.

# Structural Optimization and Performance Analysis of Honeycomb Fenders in Maritime Applications

P. R. Udupi, A. Thomas, J. Jovanova  
Delft University of Technology

**Abstract**—This thesis explores improving energy absorption in PVC air-filled boat fenders by integrating twisted honeycomb lattice structures. The research addresses key issues in current fender designs, aiming to enhance energy dissipation. Using metamaterial design, the study examines different twist angles in honeycomb patterns. A 20° twist optimizes energy absorption by balancing compression and shear forces, while higher angles like 30° add stiffness, reducing efficiency. Simulations in ANSYS Workbench reveal a structural activation threshold at 10°. These findings offer insights for advancing fender design and marine applications.

## INTRODUCTION

In maritime operations, fenders are crucial components that act as cushioning devices between vessels and docking structures, or between vessels themselves. Their primary function is to absorb the kinetic energy generated during berthing and mooring, which helps prevent damage to both vessels and dock infrastructure. By distributing impact forces and minimizing structural damage, fenders play an essential role in maintaining the integrity of maritime assets [1]. Traditional fenders are commonly made from materials such as foam, rubber, or air-filled PVC. While these materials are initially effective in energy absorption, they often suffer from plastic deformation, wear, and inconsistent performance under extreme conditions, leading to frequent replacements and increased waste. PVC-based fenders, in particular, demonstrate variability in energy dissipation, which has exposed a

significant research gap in optimizing fender designs for better durability and performance [1], [4].

The ability of fenders to absorb energy efficiently depends on the materials and designs employed. Traditional materials, while widely used, fall short in maximizing energy absorption under dynamic loads. This limitation has spurred interest in advanced materials and designs, particularly metamaterials. Metamaterials, with their engineered microstructures, offer unique properties like enhanced toughness and negative Poisson's ratios, which are not found in conventional materials [2]. These innovative materials can improve energy absorption and recovery, making them ideal for fender applications where impact resilience is critical. Furthermore, metamaterials with honeycomb lattice structures have been identified as particularly promising for maritime fender systems, offering improved structural integrity and energy absorption capabilities while reducing environmental impact by decreasing



**FIGURE 1.** Figure Illustrating a Standard Air-Filled Fender

material waste and enhancing durability [3].

Honeycomb structures, like those found in beehives, offer a natural model for optimal material usage, balancing lightness and structural integrity. The hexagonal configuration minimizes material while maximizing space utilization, a concept known as the honeycomb conjecture [5]. Such structures have been widely adopted in engineering applications, from aerospace to automotive industries, due to their superior energy absorption and mechanical properties [6].

Cellular materials, including foams and honeycombs, are a class of lightweight structures with excellent energy absorption capabilities, making them ideal for various structural applications [8]. Honeycombs, in particular, have a two-dimensional, periodic cellular structure that can be engineered for different geometries, such as hexagonal, triangular, or circular, allowing for flexibility in mechanical performance [9], [10]. The ability to fine-tune microstructural parameters like density and cell wall thickness further enhances their energy-absorbing potential [11].

The mechanical behavior of honeycombs is largely dependent on their microstructural design, which can lead to unique properties such as a negative Poisson's ratio (NPR) and negative stiffness. These properties are a result of the material's structural topology, rather than its intrinsic composition, providing superior fracture toughness and impact resistance [13], [12]. Inspired by natural structures, these configurations have been studied extensively for their potential in advanced structural applications [6].

The development of boat fenders has played a crucial role in enhancing maritime safety by preventing collision damage during docking and mooring operations. Early fenders, made from woven ropes and natural materials, served as rudimentary barriers, relying on their physical bulk to absorb impact. However, as maritime traffic increased and ships grew larger, more effective energy absorption methods became necessary. This led to the introduction of synthetic materials like rubber and plastic in the 20th century, revolutionizing fender technology by improving durability and impact resistance. As a result, more sophisticated fender designs, such as cylindrical, D-shape, and arch fenders, emerged to cater to diverse vessel types and docking conditions [18].

Fender technology continued to evolve, with advancements focusing not just on materials but also on the geometric optimization of fenders to maximize energy absorption. By examining the complexities of berthing energy, modern fender systems are now designed to absorb substantial impact forces, ensuring the protection of both the vessel and dock infrastructure [19]. Today's fenders are highly engineered systems, combining historical practices with modern materials and designs that emphasize factors like softness coefficients and energy dissipation capabilities [20].

Air-filled pneumatic fenders are widely used due to their ability to cushion vessels against various compression forces during docking. These fenders utilize compressed air as a medium, making them highly adaptable to different docking scenarios, as they can handle both normal and angular compression, thus providing reliable protection in various conditions [21].

The ongoing evolution of boat fender technology mirrors broader advancements in energy absorption across multiple industries. Concepts of energy dissipation, such as the conversion of kinetic energy into inelastic forms like plastic deformation, are key to improving safety and minimizing damage during impacts [23], [25]. By applying principles such as controlling deformation modes and ensuring lightweight yet high energy-absorption capacity, fender designs continue to be optimized for superior performance [24].

Biomimicry offers a framework for deriving innovative engineering solutions from natural systems. In this project, inspiration is drawn from the spiral structure of eland horns and the overlapping scales of the pangolin to enhance impact-absorbing designs. The spiral horns of the eland (*Taurotragus oryx*) are



a vital adaptation used in combat, where the twisting motion during interlocking reduces direct impact forces. This design helps distribute stress along the length of the horn, minimizing potential damage and protecting the skull from high-impact forces [26], [27]. The same principle can be applied to engineered structures, providing enhanced energy dissipation and stress management.

Pangolin scales, composed of a combination of  $\alpha$  and  $\beta$  keratins, offer another model for biomimicry, particularly in their crossed-lamellar structure, which exhibits remarkable toughness and impact resistance. These overlapping scales provide multidirectional support and maintain mechanical strength while absorbing impacts from various angles [28], [29]. Their internal keratin lamellae are nearly parallel to the surface but tilt inward at approximately  $45^\circ$ , promoting crack deflection and enhancing fracture resistance [31]. This design concept, with its ability to deform without fracturing under compressive loads, can inspire the creation of materials that distribute stress efficiently across their surfaces [30].

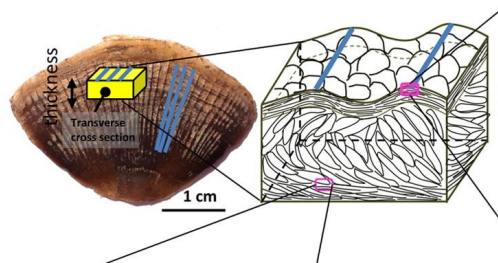


**FIGURE 2.** Figure of keratin lamellae twist [7]

## METHODOLOGY

The methodology of this study is aimed at comparing the performance of traditional air-filled boat fenders with hybrid fenders, which integrate both air and honeycomb structures made from PVC. The primary goal is to assess and optimize the energy absorption capabilities of these fender designs. To achieve this, the fenders were modeled in SolidWorks and imported into ANSYS Workbench, where explicit dynamic simulations were conducted to test their performance under various impact conditions. This systematic approach ensures uniformity across assessments and evaluates the structural integrity and energy absorption of each fender design under realistic docking and collision scenarios.

The focus of the study is on geometric modifications rather than material changes, maintaining PVC as the primary material to isolate the impact of design improvements. By optimizing the internal structure, such as incorporating honeycomb cells, the design aims to improve energy absorption and load distribution. The physical properties of PVC, including density, Young's modulus, and Poisson's ratio, were sourced from ANSYS simulations and used to ensure accurate modeling. Impact velocities ranging from 1286.11 mm/s ( $30^\circ$ ) to 2572.22 mm/s ( $90^\circ$ ) were considered to simulate both controlled and uncontrolled docking scenarios, providing a comprehensive assessment of fender performance under diverse conditions [35].

The base fender, constructed with a 5 cm thick cross-section, was selected based on industry standards and optimized for computational efficiency. The fender had a diameter of 25 cm and a length of 80 cm, representing a standard size used in practical applications [36]. A wall thickness of 3.5 mm was chosen for the base model to match the weight and dimensions of a typical fender. The air pressure inside the fender was set to 2 psi, as recommended by manufacturers, to simulate real-world conditions [37]. The primary energy absorption mechanism in this model is air compression, where the internal air compresses upon impact, allowing the fender to deform and dissipate the collision energy.

To enhance the design, internal honeycomb structures were incorporated into the base model. The wall thickness was reduced to 2 mm to prevent weight increase while maintaining strength. The air compression, combined with the mechanical resilience of the honeycomb structures, creates a dual-method system for energy absorption. The honeycomb cells provide additional structural support, allowing the fender to absorb more impact energy while maintaining flexibility and preventing blockages from external debris. This hybrid design improves the fender's ability to deform efficiently and distribute stress across the structure.

Finally, a series of enhanced designs introduced twisted honeycomb structures, starting with a  $5^\circ$  twist angle. This modification is intended to explore torsional effects as an additional energy absorption mechanism, inspired by the natural misalignment observed in pangolin scales. This triple-method system, which combines air compression, honeycomb structure resilience, and torsional deformation, is expected to further improve energy absorption and reduce crack propagation, ensuring the longevity and durability of



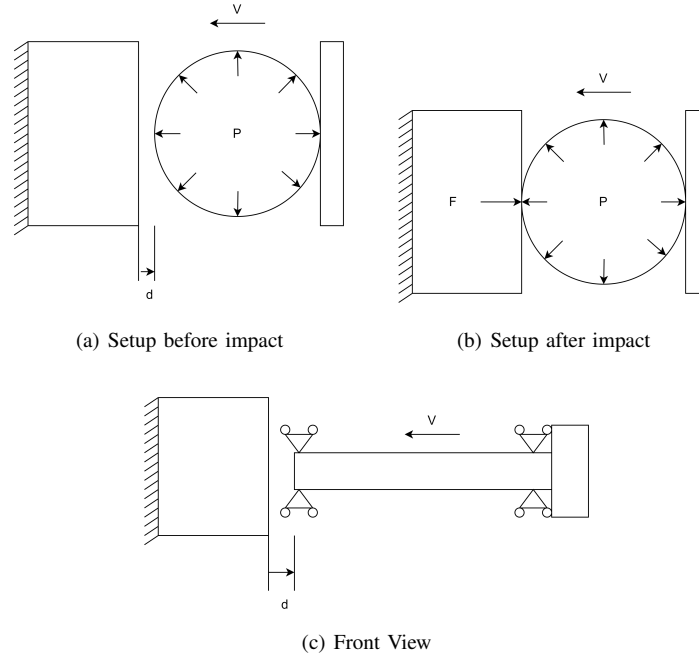


FIGURE 3. Simulation Setup

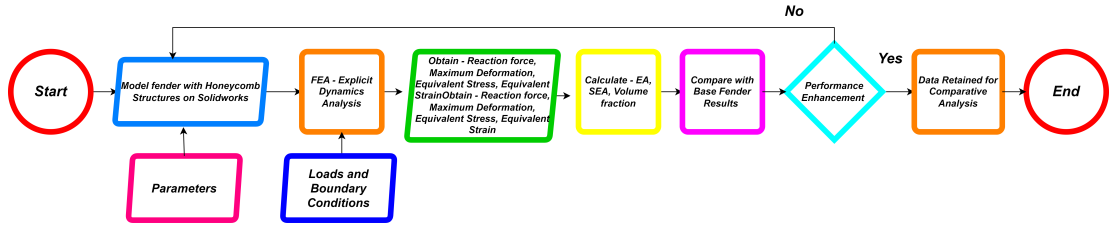


FIGURE 4. Overview of the Employed Design Process

the fender design. The combination of these design innovations provides a more effective solution for impact resistance, with potential applications in a wide range of docking and collision scenarios.

### Key Performance Metrics

Key performance metrics compare the base fender with test samples to identify improvements:

- **Energy Absorption Capability (EA):** Measures how well the fender protects vessels from impact damage, calculated as:

$$EA = \int_0^d F ds \quad (1)$$

- **Specific Energy Absorption Capability (SEA):** Indicates efficiency in absorbing impact energy rel-

ative to mass, calculated as:

$$SEA = EA/m \quad (2)$$

- **Volume Fraction:** The ratio of the base fender's volume to the test sample's volume, with optimized designs indicating material efficiency:

$$Vol_{frac} = Vol_{base}/Vol_{sample} \quad (3)$$

Ideally,  $Vol_{frac} = 1$  or  $Vol_{frac} > 1$

- **Stress Distribution:** Evaluates how internal forces distribute during impacts, focusing on von Mises stress to ensure the design's stability and integrity under load.

## RESULTS AND DISCUSSIONS

Initial experiments applying a  $5^\circ$  twist to the honeycomb lattice structure failed to improve energy

**TABLE 1.** Table showing the results of the Enhanced Dual-Method Samples

	<i>EA</i>	<i>SEA</i>	<i>Volume Fraction</i>	<i>Max Stress</i>
<i>Base Fender</i>	0.1334 J	0.7278 J/kg	1	0.3006 MPa
<i>5°</i>	0.6388 J	1.6488 J/kg	0.4718	0.48859 MPa
<i>10°</i>	1.1590 J	3.0170 J/kg	0.4758	0.74833 MPa
<i>15°</i>	1.3762 J	3.6429 J/kg	0.4838	1.2758 MPa
<i>20°</i>	2.3252 J	6.1357 J/kg	0.4823	2.4668 MPa
<i>25°</i>	1.6585 J	4.4752 J/kg	0.4932	1.9658 MPa
<i>30°</i>	3.3241 J	9.0272 J/kg	0.4964	1.5039 MPa
<i>35°</i>	1.1601 J	3.1252 J/kg	0.4924	2.241 MPa
<i>40°</i>	1.8765 J	5.0302 J/kg	0.4899	2.9961 MPa

absorption and actually performed worse than the dual method system without twisting. The energy absorption (EA) at 0° was approximately 0.98 Joules, compared to only 0.63 Joules at a 5° twist, as shown in Table 1. This decline in performance is likely due to a structural activation threshold, where the minimal 5° twist was insufficient to fully engage the deformation mechanism intended to enhance energy absorption. The geometry of the honeycomb lattice appears to require a larger angle to effectively redistribute stress and activate the structural transformations needed to improve performance.

Energy absorption increased with larger twist angles, particularly between 10° and 20°, as illustrated in figure 6. At these angles, the honeycomb structures deformed more efficiently under impact, as the combination of compression and shear forces compacted the cells and air pockets more effectively. This optimal performance at 20° resulted from the interplay between elastic and torsional deformation, which enhanced the fender's capacity to absorb energy. Beyond 20°, however, localized buckling occurred in certain honeycomb cells, leading to less uniform deformation and fluctuations in energy absorption. The 20° twist represents a critical threshold, maximizing energy absorption through a balance of structural compaction and stress distribution across the fender.

At this optimal angle, torsional deformation introduced by twisting the honeycomb enhances shear stress distribution, aligning internal forces to manage compressive loads efficiently. This deformation creates well-defined load pathways, allowing the fender to distribute stress evenly and prevent localized concentrations, which could otherwise lead to material fatigue or failure. The uniform stress field at 20° improves the resilience of the fender, promoting both torsional and elastic deformation modes that ensure efficient energy dissipation while maintaining structural integrity.

However, increasing the twist to 30° achieved maximum energy absorption but introduced limita-

tions. Simulations showed a non-uniform deformation pattern, where only the cells near the impact site experienced significant compression, leading to uneven force distribution. Additionally, the force-displacement curve exhibited a plateau, indicating that the material was approaching its energy absorption limit. This suggests that while the 30° twist is effective for handling sustained impacts, it may result in increased stiffness and reduced flexibility, compromising the structure's ability to absorb further loads if unexpected or excessive forces are applied. Consequently, the 30° twist presents a trade-off between absorption efficiency and structural adaptability.

## CONCLUSION

This project explored the enhancement of traditional air-filled boat fenders by integrating honeycomb lattice structures to improve energy absorption while retaining PVC as the base material. The study focused on optimizing energy dissipation, with hybrid designs combining air and honeycomb structures showing superior performance compared to traditional PVC fenders. A critical structural activation threshold was identified at 10° of twist, where energy absorption began to increase, reaching peak efficiency at 20°. Beyond this point, further twisting led to localized buckling, reducing uniformity in energy absorption. While the 30° twist enhanced absorption initially, it introduced excessive stiffness and uneven stress distribution. The findings highlight the importance of balancing structural flexibility and energy management, with the 20° twist being optimal for maximizing energy absorption.

## Future Works

For future research efforts, the initial step involves enhancing simulation models to incorporate multi-directional impact scenarios. This will better capture the diverse response behaviors of fenders under realistic docking conditions and provide a more accurate assessment of their performance. Following

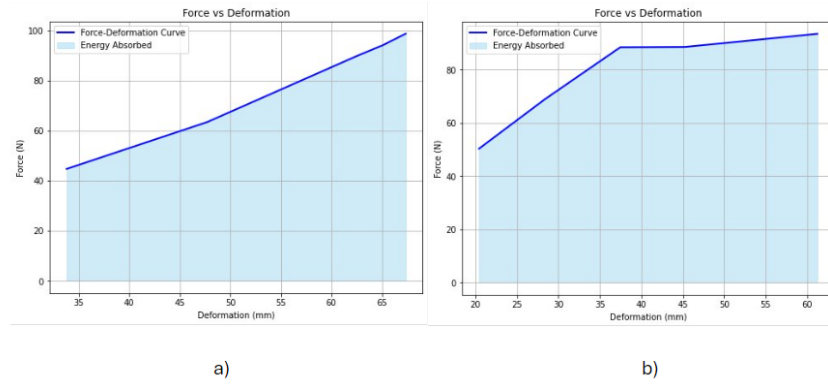


**FIGURE 5.** Force vs Deformation Graph of a) 20° twist b) 30° twist

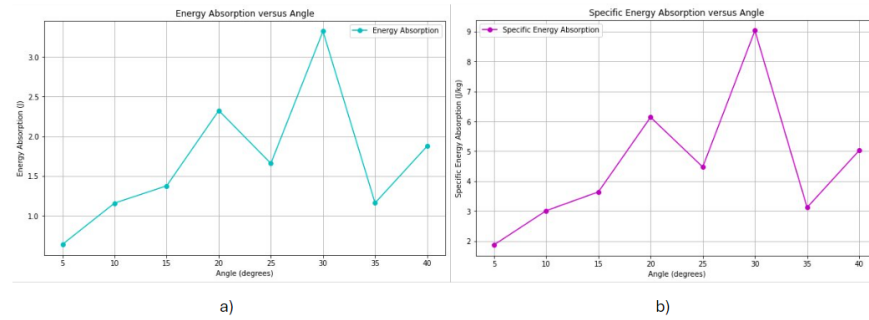


**FIGURE 6.** a) EA vs Angle b) SEA vs Angle

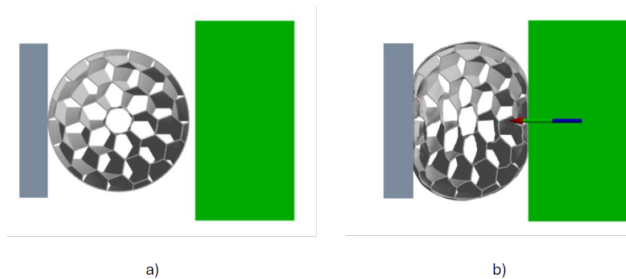


**FIGURE 7.** Cross section of the Enhanced Dual Method 20° sample a) before impact b) after impact

this simulation refinement, fabricating a prototype for comprehensive testing is crucial to evaluate its performance under realistic conditions. This testing will help identify any discrepancies between simulation results and actual performance, offering an opportunity to refine the model and approach. Subsequently, conducting fatigue analysis is essential to assess the long-term viability and resilience of the fender design under cyclic loading conditions. Comparing results from the base fender and the enhanced 20° model will provide further insights into the effectiveness of design

modifications.

## ACKNOWLEDGMENTS

I would like to express my deepest gratitude to my supervisors, Dr. Jovana Jovanova and Amy Thomas, for their continuous guidance, encouragement, and invaluable insights throughout the course of this research. Their expertise and support were instrumental in shaping this project, and I am deeply appreciative of their mentorship.

I would also like to thank the faculty and staff of the Mechanical Engineering Department at TU Delft for providing an inspiring academic environment and access to the resources necessary for this work. Finally, I extend my heartfelt thanks to my family and friends for their unwavering support and encouragement throughout my master's journey.

## REFERENCES

1. T. E. Spencer, "Marine fender systems," in *Ports 2004: Port Development in the Changing World*, pp. 1–10, 2004.

2. A. Yousefi, S. Jolaiy, M. L. Dezaki, A. Zolfagharian, A. Serjouei, and M. Bodaghi, "3D-Printed Soft and Hard Meta-Structures with Supreme Energy Absorption and Dissipation Capacities in Cyclic Loading Conditions," *Adv. Eng. Mater.*, vol. 25, no. 4, pp. 2201189, 2023, Wiley.
3. M. Bodaghi, N. Namvar, A. Yousefi, H. Teymouri, F. Demoly, and A. Zolfagharian, "Metamaterial boat fenders with supreme shape recovery and energy absorption/dissipation via FFF 4D printing," *Smart Mater. Struct.*, vol. 32, no. 9, pp. 095028, 2023, IOP Publishing.
4. A. Escorsell, "How many fenders do I need for my boat? - A complete guide," Online: <https://www.sail-world.com/news/252339/How-many-fenders-do-I-need-for-my-boat>, accessed Oct. 4, 2022.
5. T. C. Hales, "The honeycomb conjecture," *Discrete Comput. Geom.*, vol. 25, pp. 1–22, 2001, Springer.
6. C. Qi, F. Jiang, and S. Yang, "Advanced honeycomb designs for improving mechanical properties: A review," *Compos. Part B: Eng.*, vol. 227, pp. 109393, 2021, Elsevier.
7. B. Wang, W. Yang, V. R. Sherman, and M. A. Meyers, "Pangolin armor: overlapping, structure, and mechanical properties of the keratinous scales," *Acta Biomater.*, vol. 41, pp. 60–74, 2016, Elsevier.
8. H. Yu, Z. Guo, B.
9. S. Malek and L. Gibson, "Effective elastic properties of periodic hexagonal honeycombs," *Mechanics of Materials*, vol. 91, pp. 226–240, 2015, Elsevier.
10. J. Chung and A. M. Waas, "Compressive response of circular cell polycarbonate honeycombs under inplane biaxial static and dynamic loading. Part I: experiments," *International Journal of Impact Engineering*, vol. 27, no. 7, pp. 729–754, 2002, Elsevier.
11. L. J. Gibson, "Cellular solids," *Mrs Bulletin*, vol. 28, no. 4, pp. 270–274, 2003, Cambridge University Press.
12. Q. Zhang and H. Liu, "On the dynamic response of porous functionally graded microbeam under moving load," *International Journal of Engineering Science*, vol. 153, p. 103317, 2020, Elsevier.
13. C. Quan, B. Han, Z. Hou, Q. Zhang, X. Tian, and T. J. Lu, "3D printed continuous fiber reinforced composite auxetic honeycomb structures," *Composites Part B: Engineering*, vol. 187, p. 107858, 2020, Elsevier.
14. C. Körner, "Cellular mechanical metamaterials," Online: <https://www.wtm.tf.fau.eu/forschung/additive-fertigung/cellular-mechanical-metamaterials/>, accessed Oct. 4, 2022.
15. T. Lund, "How to Tie Fenders on a Boat," Online: <https://www.wikihow.com/Tie-Fenders-on-a-Boat>, accessed Sept. 16, 2021.
16. Lion Rubber, "Tyre Fender," Online: <https://lionrubber.com/products/lion-tug-boat-fenders/tyre-fender/>, accessed 2024.
17. G. Cubitt, A. Mishra, and E. Bussiere, "What is a pangolin?," Online: <https://www.savepangolins.org/what-is-a-pangolin>, accessed 2022.
18. S. Ueda, T. Hirano, S. Shiraishi, S. Yamamoto, and S. Yamase, "Reliability design method of fender for berthing ship," in *Int. Navigation Congress (30th: 2002: Sydney, NSW)*, pp. 692–707, 2002, Institution of Engineers Sydney, NSW.
19. M. S. Atiq, A. K. Shajib, and others, "Analysis of Marine Fender Systems Minimizing the Impact of Collision Damage," in *Proc. 13th Int. Conf. Marine Technology (MARTEC 2022)*, 2023.
20. A. Roubos, D. J. Peters, L. Groenewegen, and R. Steenbergen, "Partial safety factors for berthing velocity and loads on marine structures," *Marine Structures*, vol. 58, pp. 73–91, 2018, Elsevier.
21. S. Sakakibara and M. Kubo, "Ship berthing and mooring monitoring system by pneumatic-type fenders," *Ocean Eng.*, vol. 34, no. 8-9, pp. 1174–1181, 2007, Elsevier.
22. W. Johnson and S. R. Reid, "METALLIC ENERGY DISSIPATING SYSTEMS," *Appl. Mech. Rev.*, vol. 31, no. 3, pp. 277–288, Jan. 1978, ASME.
23. W. Johnson, "The elements of crashworthiness: scope and actuality," *Proc. Inst. Mech. Eng. Part D: J. Automobile Eng.*, vol. 204, no. 4, pp. 255–273, 1990, Sage Publications.
24. E. W. Andrews, L. J. Gibson, and M. F. Ashby, "The creep of cellular solids," *Acta Materialia*, vol. 47, no. 10, pp. 2853–2863, 1999, Elsevier.
25. G. Lu and T. X. Yu, *Energy absorption of structures and materials*, Elsevier, 2003.
26. L. Trestan, R. Jung, T. Jrab, and V. Novakov, "Mechanical Analysis of Animal Horns."
27. J. Cappelli, A. J. García, R. Kotrba, P. G. Pozo, T. Landete-Castillejos, L. Gallego, and F. Ceacero, "The bony horncore of the common eland (*Taurotragus oryx*): composition and mechanical properties of a spiral fighting structure," *J. Anatomy*, vol. 232, no. 1, pp. 72–79, 2018, Wiley.
28. M. Briggs and P. Briggs, *The encyclopedia of world wildlife*, Parragon Publishing India, 2006.
29. Y. Seki, B. Kad, D. Benson, and M. A. Meyers, "The toucan beak: structure and mechanical response,"

- Mater. Sci. Eng.: C*, vol. 26, no. 8, pp. 1412–1420, 2006, Elsevier.
30. L. Tombolato, E. E. Novitskaya, P. Y. Chen, F. A. Sheppard, and J. McKittrick, "Microstructure, elastic properties and deformation mechanisms of horn keratin," *Acta Biomaterialia*, vol. 6, no. 2, pp. 319–330, 2010, Elsevier.
  31. Z. Liu, M. A. Meyers, Z. Zhang, and R. O. Ritchie, "Functional gradients and heterogeneities in biological materials: Design principles, functions, and bioinspired applications," *Prog. Mater. Sci.*, vol. 88, pp. 467–498, 2017, Elsevier.
  32. S. R. Reid and C. Peng, "Dynamic uniaxial crushing of wood," *Int. J. Impact Eng.*, vol. 19, no. 5-6, pp. 531–570, 1997, Elsevier.
  33. M. Esgandari and O. Olatunbosun, "Implicit–explicit co-simulation of brake noise," *Finite Elements in Analysis and Design*, vol. 99, pp. 16–23, 2015, Elsevier.
  34. S. Yao, Y. Zhou, Z. Li, P. Zhang, Y. Cao, and P. Xu, "Energy absorption characteristics of square frustum lattice structure," *Composite Structures*, vol. 275, p. 114492, 2021, Elsevier.
  35. A. Roubos, L. Groenewegen, and D. J. Peters, "Berthing velocity of large seagoing vessels in the port of Rotterdam," *Marine Structures*, vol. 51, pp. 202–219, 2017, Elsevier.
  36. Majoni, "SPORTDEAL," [Online]. Available: <https://www.sportdeal.nl/classic-cilinder-fenders-zwart-alle-matenc-8712256001039+size-10~x~42~cm>. Accessed: Oct. 2018.
  37. Taylor-Made, "Fender & Buoy: Inflation Instructions," [Online]. Available: [https://defender.com/assets/pdf/taylor-made/taylor\\_inflate.pdf](https://defender.com/assets/pdf/taylor-made/taylor_inflate.pdf). Accessed: 2017.
  38. N. Y. Gnedin, V. A. Semenov, and A. V. Kravtsov, "Enforcing the Courant–Friedrichs–Lewy condition in explicitly conservative local time stepping schemes," *Journal of Computational Physics*, vol. 359, pp. 93–105, 2018, Elsevier.
  39. R. Courant, K. Friedrichs, and H. Lewy, "Über die partiellen Differenzengleichungen der mathematischen Physik," *Mathematische Annalen*, vol. 100, no. 1, pp. 32–74, 1928, Springer.